Stem Cell Reports
Article
OPEN ACCESS

GATA Factor-G-Protein-Coupled Receptor Circuit Suppresses Hematopoiesis

Xin Gao,[1] Tongyu Wu,[1] Kirby D. Johnson,[1] Jamie L. Lahvic,[2] Erik A. Ranheim,[3] Leonard I. Zon,[2] and Emery H. Bresnick[1,*]

[1]UW-Madison Blood Research Program, Department of Cell and Regenerative Biology, Carbone Cancer Center, University of Wisconsin School of Medicine and Public Health, Madison, WI 53705, USA
[2]Stem Cell Program and Division of Hematology/Oncology, Children's Hospital and Dana Farber Cancer Institute, Howard Hughes Medical Institute, Harvard Medical School, Harvard Stem Cell Institute, Stem Cell and Regenerative Biology Department, Harvard University, Boston, MA 02114, USA
[3]Department of Pathology, University of Wisconsin School of Medicine and Public Health, Madison, WI 53705, USA
*Correspondence: ehbresni@wisc.edu
http://dx.doi.org/10.1016/j.stemcr.2016.01.008

SUMMARY

Hematopoietic stem cells (HSCs) originate from hemogenic endothelium within the aorta-gonad-mesonephros (AGM) region of the mammalian embryo. The relationship between genetic circuits controlling stem cell genesis and multi-potency is not understood. A *Gata2 cis* element (+9.5) enhances *Gata2* expression in the AGM and induces the endothelial to HSC transition. We demonstrated that GATA-2 rescued hematopoiesis in $+9.5^{-/-}$ AGMs. As G-protein-coupled receptors (GPCRs) are the most common targets for FDA-approved drugs, we analyzed the GPCR gene ensemble to identify GATA-2-regulated GPCRs. Of the 20 GATA-2-activated GPCR genes, four were GATA-1-activated, and only *Gpr65* expression resembled *Gata2*. Contrasting with the paradigm in which GATA-2-activated genes promote hematopoietic stem and progenitor cell genesis/function, our mouse and zebrafish studies indicated that GPR65 suppressed hematopoiesis. GPR65 established repressive chromatin at the +9.5 site, restricted occupancy by the activator Scl/TAL1, and repressed *Gata2* transcription. Thus, a *Gata2 cis* element creates a GATA-2-GPCR circuit that limits positive regulators that promote hematopoiesis.

INTRODUCTION

Establishment and maintenance of the adult hematopoietic system requires the generation of hematopoietic stem cells (HSCs) from a unique endothelial cell (hemogenic) in the aorta-gonad-mesonephros (AGM) region of the mammalian embryo (Dzierzak and Speck, 2008). HSCs develop in clusters that bud off from hemogenic endothelium (Bertrand et al., 2010; Boisset et al., 2010), a process termed endothelial to hematopoietic transition (EHT). HSCs migrate to and colonize the fetal liver and, subsequently, the bone marrow (Orkin and Zon, 2008). Whereas major efforts have focused on defining regulatory proteins/networks governing EHT, many questions remain unanswered regarding the molecular constituents and mechanisms.

Master regulatory transcription factors co-localize at *cis* elements of target genes in hematopoietic stem and progenitor cells (HSPCs) to establish genetic networks that control hematopoiesis (Beck et al., 2013; Fujiwara et al., 2009; May et al., 2013; Tripic et al., 2008; Wilson et al., 2010; Wozniak et al., 2008; Yu et al., 2009). The combinatorial mechanisms operating in hemogenic endothelium, and the relationship between mechanisms governing EHT and HSC multi-potency, are unclear. A shared component of the mechanisms involves the transcription factor GATA-2, which is required for definitive hematopoiesis (Tsai et al., 1994). GATA-2 functions in hemogenic endothelium to induce EHT and regulates HSC function (de Pater et al., 2013; Gao et al., 2013; Johnson et al., 2012; Ling et al., 2004; Rodrigues et al., 2005).

Since GATA-2 induces EHT, it is instructive to consider factors/signals upstream of GATA-2. Deletion of a *cis* element 9.5 kb downstream of the *Gata2* promoter (+9.5) in mice decreased *Gata2* expression in AGM hemogenic endothelium, deregulated genes encoding positive regulators of hematopoiesis, and abrogated EHT (Gao et al., 2013). Deletion of a *cis* element 77 kb upstream of the promoter (−77) reduced *Gata2* expression in myelo-erythroid progenitors and impaired progenitor function without affecting EHT (Johnson et al., 2015). The defective HSC generator of $+9.5^{-/-}$ embryos depleted HSPCs in the fetal liver and caused lethality at embryonic day 13–14 (E13–14) (Johnson et al., 2012). Since the +9.5 controls *Gata2* expression and EHT (Gao et al., 2013; Hsu et al., 2013), and GATA-2 occupies the +9.5 (Fujiwara et al., 2009; Grass et al., 2006), one aspect of the +9.5 mechanism involves GATA-2-mediated positive autoregulation. Factors implicated upstream of GATA-2 include bone morphogenetic protein 4 (Lugus et al., 2007; Maeno et al., 1996), Notch signaling (Guiu et al., 2013; Robert-Moreno et al., 2008), the Ets factor Etv2 (Liu et al., 2015), and the methylcytosine dioxygenases Tet2/Tet3 (Li et al., 2015).

The *Gata2* +9.5 site regulates a large gene cohort in hemogenic endothelium, and these genes do not parse into a single pathway (Gao et al., 2013). The genes include

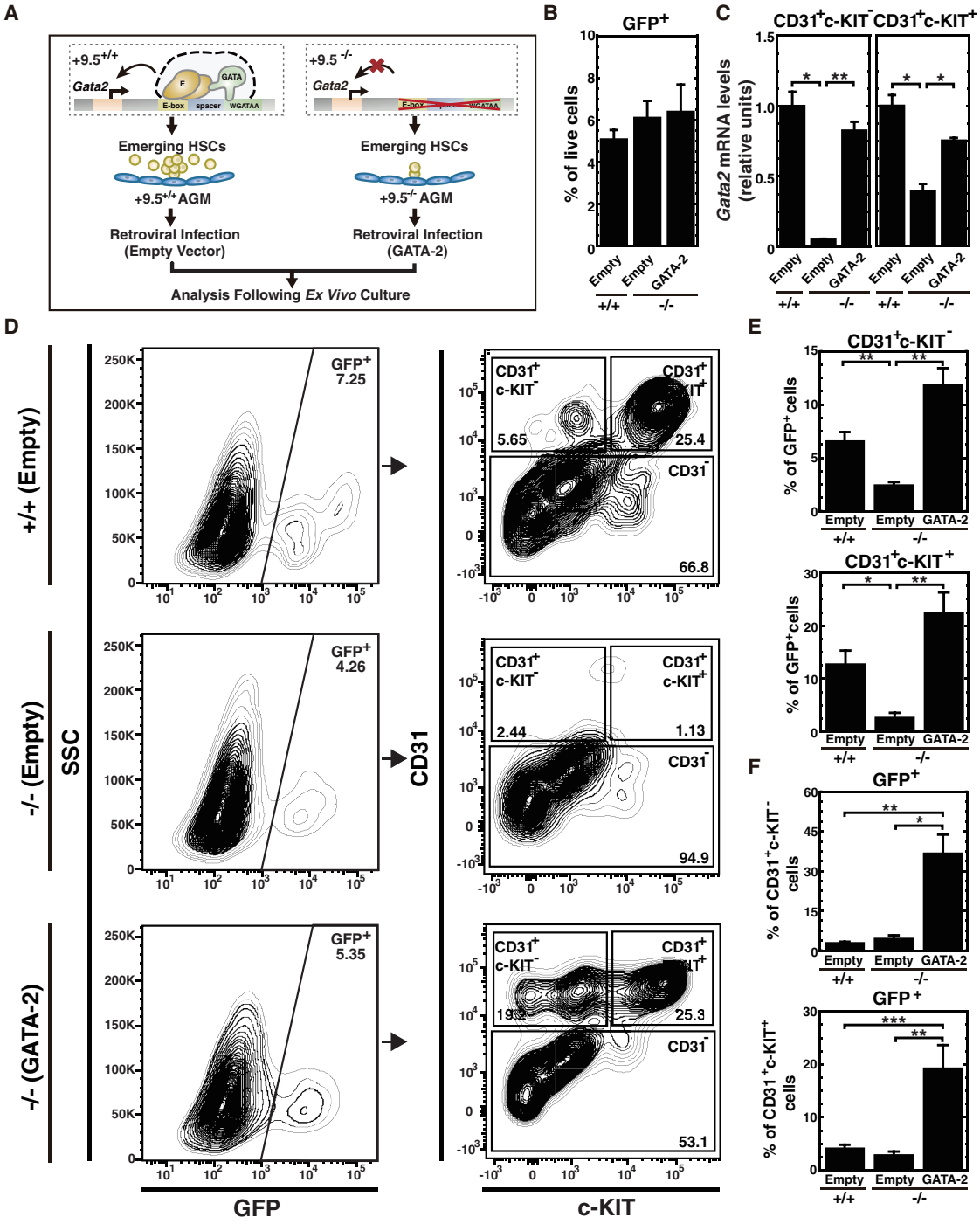

Figure 1. GATA-2 Expression in +9.5$^{-/-}$ AGM Rescues CD31^{+}c-KIT^{+} Hematopoietic and CD31^{+}c-KIT^{-} Endothelial Cells

(A) AGM ex vivo retroviral infection and culture.

(B) Flow cytometric analysis of GFP^{+} cells within total live cells (6 litters: +9.5$^{+/+}$-Empty [n = 8 embryos]; +9.5$^{-/-}$-Empty [n = 4 embryos]; +9.5$^{-/-}$-GATA-2 [n = 6 embryos]).

(C) RT-PCR analysis of *Gata2* mRNA levels in FACS-sorted CD31^{+}c-KIT^{-} and CD31^{+}c-KIT^{+} cells (six litters: +9.5$^{+/+}$-Empty [n = 8 embryos]; +9.5$^{-/-}$-Empty [n = 4 embryos]; +9.5$^{-/-}$-GATA-2 [n = 6 embryos]).

(D) Representative flow cytometric plots of CD31^{+}c-KIT^{+} and CD31^{+}c-KIT^{-} cell populations in infected AGMs after 96 hr of ex vivo culture.

(legend continued on next page)

Runx1, *Lyl1*, and *Mpl*, positive mediators of HSC generation and/or function. The identification of vital constituents of the +9.5-dependent genetic network will reveal how a *cis* element triggers EHT. As GATA-2 lacks features that can be leveraged for drug binding, identifying +9.5 network components will reveal strategies to promote HSC generation/function for transplantation and inhibit leukemia cell proliferation and survival.

The most common targets for drugs approved by the Food and Drug Administration are GPCRs (Roth and Kroeze, 2015). The GPCR family consists of 341 non-olfactory receptors classified as rhodopsin, secretin, glutamate, adhesion, and frizzled/taste2, based on sequence homology (Lagerstrom and Schioth, 2008). CXCR4, a rhodopsin-like GPCR, recognizes SDF-1/CXCL-12 and controls HSPC survival, proliferation, migration, and engraftment (Broxmeyer et al., 2005). CXCR4 antagonists are used as mobilizing agents for stem cell transplantation. The prostaglandin PGE2, which functions through a group of related GPCRs (Sugimoto and Narumiya, 2007), expands HSPCs (Goessling et al., 2011; Hoggatt et al., 2013; North et al., 2007). We described +9.5-mediated upregulation of *Gpr56* expression (Gao et al., 2013). Loss-of-function analyses indicated that GPR56 promotes EHT (Solaimani Kartalaei et al., 2015) and contributes to HSC maintenance (Saito et al., 2013). Galpha(s)-mediated signaling controls HSPC engraftment of bone marrow (Adams et al., 2009).

By profiling expression of the GPCR cohort in the AGM, we discovered a subset of GATA-2-regulated GPCRs and a GATA-2- and GATA-1-regulated cohort, including GPR65, which suppresses AGM hematopoiesis. The +9.5 site, and its regulated protein GATA-2, which positively regulate hematopoiesis, upregulated *Gpr65* encoding a negative regulator of hematopoiesis. These results provide evidence for a GATA factor-GPCR type I incoherent feedforward loop as a vital component of the genetic network that controls HSPC generation and function.

RESULTS

GATA-2 Expression in +9.5$^{-/-}$ AGM Rescues Hematopoiesis

Deletion of the +9.5 site reduced *Gata2* expression in AGM hemogenic endothelium and abrogated EHT (Gao et al., 2013) (Figure 1A). These results suggest that factors/signals conferring +9.5 activity control *Gata2* expression, which promotes EHT. In principle, the +9.5 might regulate other genes in *cis* or in *trans* that control EHT. To determine whether the HSC generation defect of +9.5$^{-/-}$ AGM results from insufficient GATA-2 production, we tested whether GATA-2 expression rescues the defect. E11.5 mouse embryo AGMs were infected with GATA-2-expressing retrovirus (Figure 1A). After 96 hr of explant culture, we quantitated endothelial and hematopoietic cell populations in infected (GFP$^+$) cells by flow cytometry using CD31 and c-KIT surface markers. The infection efficiency was similar among the three conditions (+9.5$^{+/+}$-empty vector, +9.5$^{-/-}$-empty vector, +9.5$^{-/-}$-GATA-2), as indicated by the indistinguishable percentage of GFP$^+$ live cells (Figure 1B). GATA-2 expression restored *Gata2* mRNA to the wild-type level in CD31$^+$c-KIT$^-$ endothelial and CD31$^+$c-KIT$^+$ hematopoietic cells (Figure 1C), and rescued both populations (Figures 1D and 1E). Since the infected cells express GFP, the percentage of GFP$^+$ cells in each population increased in +9.5$^{-/-}$ AGM infected with GATA-2-expressing retrovirus (Figure 1F). However, retroviral-mediated GATA-2 expression did not rescue CD31$^+$c-KIT$^-$ endothelial and CD31$^+$c-KIT$^+$ hematopoietic cell populations in the GFP$^-$ cells (Figure S1). Thus, the +9.5$^{-/-}$ AGM hematopoiesis defect resulted from insufficient GATA-2 production, is associated with reduced CD31$^+$c-KIT$^-$ endothelial cells, and can be rectified by restoring GATA-2.

To assess whether the GATA-2-rescued CD31$^+$c-KIT$^+$ hematopoietic cells are functional, we measured their capacity to generate myelo-erythroid colonies in a colony-forming unit (CFU) assay. After culturing retroviral-infected AGMs for 96 hr, GFP$^+$ CD31$^+$c-KIT$^+$ hematopoietic cells were isolated by fluorescence-activated cell sorting (FACS) and assayed for their capacity to generate BFU-E (erythroid burst-forming units), CFU-GM (granulocyte, macrophage), and CFU-GEMM (granulocyte, erythrocyte, monocyte/macrophage, megakaryocyte) colonies. Whereas +9.5$^{-/-}$ AGM failed to generate CFUs, GATA-2 expression in the +9.5$^{-/-}$ AGM induced CFUs comparable with +9.5$^{+/+}$ AGM (Figure 2A). Quantification of colony types revealed comparable numbers of rescued CFU-GM colonies in comparison with wild-type AGM (Figure 2B). GATA-2 expression induced BFU-E and CFU-GEMM colonies (Figure 2B). Colonies derived from wild-type and rescued samples were morphologically indistinguishable (Figure 2C). Wright-Giemsa staining of cells from colonies revealed normal myeloid and erythroid cell generation from the GATA-2-expressing +9.5$^{-/-}$ AGM (Figure 2D). The GATA-2-induced CD31$^+$c-KIT$^+$ hematopoietic cells exhibited qualitatively and quantitatively normal activity.

(E and F) Quantitation of flow cytometry data expressed as percentage of CD31$^+$c-KIT$^-$ and CD31$^+$c-KIT$^+$ cells in GFP$^+$ cells (E) and the percentage of GFP$^+$ cells in CD31$^+$c-KIT$^-$ and CD31$^+$c-KIT$^+$ cells (F) (6 litters: +9.5$^{+/+}$-Empty [n = 8 embryos]; +9.5$^{-/-}$-Empty [n = 4 embryos]; +9.5$^{-/-}$-GATA-2 [n = 6 embryos]).

Error bars represent SEM. *p < 0.05; **p < 0.01; ***p < 0.001 (two-tailed unpaired Student's t test).

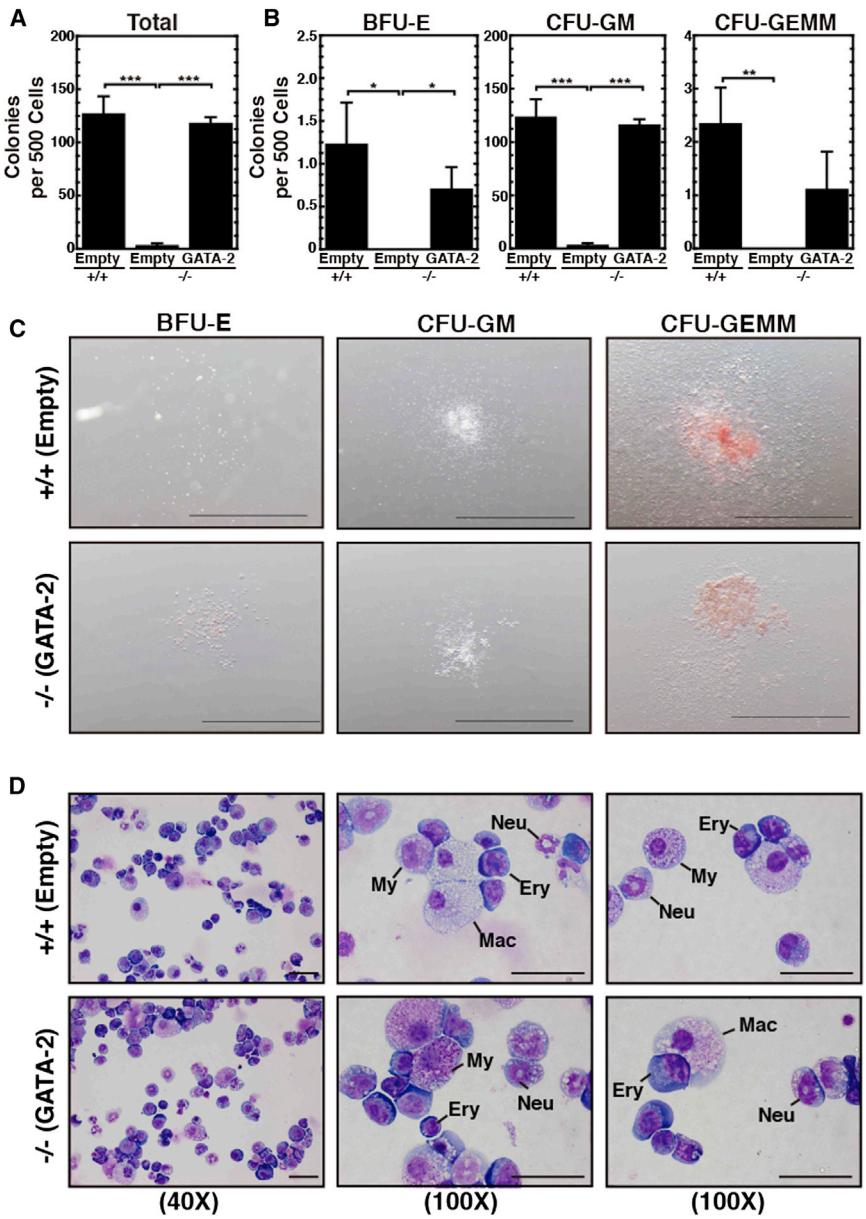

Figure 2. Rescued CD31$^+$c-KIT$^+$ Cells Exhibit Normal Colony-Forming Unit Activity

(A and B) Quantitative analysis of colony-forming activity of FACS-sorted CD31$^+$ c-KIT$^+$ cells (6 litters: +9.5$^{+/+}$-Empty [n = 9 embryos]; +9.5$^{-/-}$-Empty [n = 7 embryos]; +9.5$^{-/-}$-GATA-2 [n = 10 embryos]).

(C) Representative BFU-E, CFU-GM, and CFU-GEMM colonies from FACS-sorted CD31$^+$c-KIT$^+$ cells. Scale bar, 2 mm.

(D) Representative images of Wright-Giemsa-stained cells from colonies. Ery, erythroblast; Mac, macrophage; My, myeloid precursor; Neu, neutrophil. Scale bar, 40 μm. Error bars represent SEM. *p < 0.05; **p < 0.01; ***p < 0.001 (two-tailed unpaired Student's t test).

Global GPCR Analysis in the AGM: Discovery of a GATA Factor-Regulated GPCR Cohort

The +9.5 site confers *Gata2* expression and establishes a genetic network involving known HSC regulators and genes not implicated in hematopoiesis (Gao et al., 2013). To discover vital constituents of the network, especially those with potential for modulation by small molecules/drugs, we systematically analyzed the expression pattern of non-olfactory GPCRs (Figure 3A). The human genome encodes greater than 800 GPCRs, which are categorized into rhodopsin, secretin, glutamate, adhesion and frizzled/taste2 families based on sequence homology; 341 are distinct from the olfactory and taste GPCRs (Lagerstrom and Schioth, 2008; Roth and Kroeze, 2015). Using our AGM RNA-sequencing (RNA-seq) data (Gao et al., 2013), we parsed AGM-expressed GPCRs into the canonical categories: secretin, 5% (15); adhesion, 7% (22); glutamate, 5% (15); frizzled/taste2, 6% (20); and rhodopsin, 70% (221) (Figure 3B).

To discover GPCRs that control HSC generation and/or activity, we evaluated GPCR expression in the AGM. Of the 314 GPCRs annotated by RNA-seq, 85 were expressed at >5 transcripts per million (Figure 3C), a level that can be validated with high frequency by real-time RT-PCR. Of the 85 GPCRs, 20 were downregulated in the +9.5$^{-/-}$ AGM versus +9.5$^{+/+}$ AGM (Figure 3D),

indicating GATA-2-regulation. Using our previous microarray dataset (untreated or β-estradiol-treated G1E-ER-GATA-1 erythroid precursor cells) (DeVilbiss et al., 2013), we found that four of the 20 GATA-2-regulated GPCRs were GATA-1-regulated (Figure 3D). Our strategy refined the 314 non-olfactory, AGM-expressed GPCRs to yield *Adora3*, *Gpr65*, *Ltb4r1*, and *P2ry1*, which are GATA-2- and GATA-1-regulated.

A GATA Factor-GPCR Incoherent Feedforward Loop Suppresses AGM Hematopoiesis

As shared gene expression patterns can infer functional interconnectivity, we compared *Adora3*, *Gpr65*, *Ltb4r1*, *P2ry1*, and *Gata2* expression patterns in mouse cells and tissues. Only *Gpr65* resembled *Gata2*, both being expressed in HSPCs and mast cells (Figure S2) (http://biogps.org). As GATA-1 represses *Gata2* during erythroid maturation via a GATA switch, *Gata2* expression declines upon erythroid maturation. Mining the Erythron Database, which provides transcriptomics data during erythroid precursor cell maturation into erythrocytes (Kingsley et al., 2013), revealed *Gata2* and *Gpr65* repression upon erythroid differentiation. *Gpr65* was the only one of the four GPCR genes to have a *Gata2*-like expression pattern (Figure 3E). To further compare expression patterns, we quantitated *Gata2* and *Gpr65* mRNA in G1E-ER-GATA-1 cells treated with β-estradiol to induce erythroid maturation and in FACS-sorted R1, R2, R3, and R4/5 fetal liver cell populations. *Gpr65* and *Gata2* were repressed during erythroid maturation (Figures 3F and 3G). These correlations are consistent with GATA-2 upregulating *Gpr65* expression in the AGM and may point to a functional link between GATA-2 and GPR65. Chromatin immunoprecipitation (ChIP)-sequencing analysis in human (Figure 3H) and mouse (Figure 3I) cells revealed GATA-2 occupancy at *Gpr65*, suggesting that GATA-2 directly regulates *Gpr65* transcription. Comparison of $+9.5^{+/+}$ and $+9.5^{-/-}$ AGM revealed that reduced *Gata2* expression in the $+9.5^{-/-}$ AGM decreased *Gpr65* expression, and *Gpr65* expression was undetectable in the yolk sac (Figure 3J). Previously, we demonstrated that GATA-2 expression in mouse aortic endothelial cells increases transcription of certain GATA-2 target genes (Katsumura et al., 2014). In this system, GATA-2 increased *Gpr65* expression (Figure 3K), indicating that GATA-2 regulates *Gpr65* expression in multiple contexts. To analyze the *Gpr65* expression pattern in distinct cell types within the AGM, we mined RNA-seq data obtained with FACS-sorted endothelial cells, hemogenic endothelial cells, hematopoietic cells, and HSCs from the AGM (Solaimani Kartalaei et al., 2015). This analysis revealed that *Gpr65* is detectable in all cell types, and the levels are lower in HSCs (Figure 3L).

To test whether GPR65 controls hematopoiesis in the AGM, we conducted a loss-of-function analysis using a *Gpr65* short hairpin RNA (shRNA) retrovirus. E11.5 AGMs were infected, and after culturing for 96 hr hematopoietic cell populations were quantitated by flow cytometry. Quantitation of GFP^+ live cells indicated that control shRNA (shLuc) and sh*Gpr65* retroviruses had an indistinguishable infection efficiency (Figures 4A and 4B). *Gpr65* knockdown reduced *Gpr65* mRNA by 60%–70% (Figure 4C). While downregulating *Gpr65* did not alter $CD31^+$c-KIT^+ hematopoietic cells (Figures 4A and 4D), it increased $CD31^+$c-KIT^+SCA1^+ HSC-containing, multipotent hematopoietic cells (Figures 4A and 4E). Retroviral-mediated *Gpr65* shRNA expression did not alter $CD31^+$c-KIT^+ hematopoietic cells and $CD31^+$c-KIT^+SCA1^+ HSC-containing cells in GFP^- cells (Figure S3). These results indicate that GPR65 suppresses hematopoiesis in the AGM.

To assess whether *Gpr65* activity to suppress hematopoiesis operates in other systems, we used a morpholino (MO) targeting the *Gpr65* translation start site (*Gpr65*_ATG MO) to reduce *Gpr65* expression in zebrafish embryos. The *Gpr65*_ATG MO was injected into 1-cell stage embryos, which were analyzed for expression of the HSPC markers *Runx1/cmyb* using in situ hybridization (ISH) at 36 hr post-fertilization. The *Gpr65*_ATG MO dose-dependently increased expression of the HSPC markers *Runx1/cmyb* in the embryos (Figures 4F and 4G). A second MO, which blocks *Gpr65* splicing (*Gpr65*_SP MO), yielded an identical result; *Gpr65* downregulation induced expression of the HSPC markers *Runx1/cmyb* (Figure 4G). Thus, GPR65 suppresses hematopoiesis in mouse and zebrafish embryos.

shRNA and MO-based loss-of-function strategies may be confounded by off-target effects. As an alternative strategy we used a GPR65 antagonist, the lysosphingolipid galactosylsphingosine (psychosine). Psychosine was initially proposed to be a GPR65 agonist, based on the GPR65 requirement for psychosine-induced multi-nuclear cell formation (Im et al., 2001). Subsequently, it was demonstrated that GPR65 is a proton-sensing receptor and that psychosine antagonizes GPR65 (Radu et al., 2005; Tobo et al., 2015; Wang et al., 2004). We treated E11.5 AGMs with vehicle or psychosine, and after 96 hr, hematopoietic cells were quantitated by flow cytometry. While psychosine did not alter $CD31^+$c-KIT^+ cells (Figures 5A and 5B), it increased the $CD31^+$c-KIT^+SCA1^+ cell population, which is known to contain multipotent hematopoietic precursors (Figures 5A and 5C). In aggregate, the mouse and zebrafish studies indicate that GPR65 is an endogenous suppressor of hematopoiesis.

GPR65 Establishes Repressive Chromatin and Disrupts an Activating Complex on a *cis* Element Required for *Gata2* Transcription

To elucidate the mechanism underlying GPR65 suppression of hematopoiesis, we considered whether GPR65

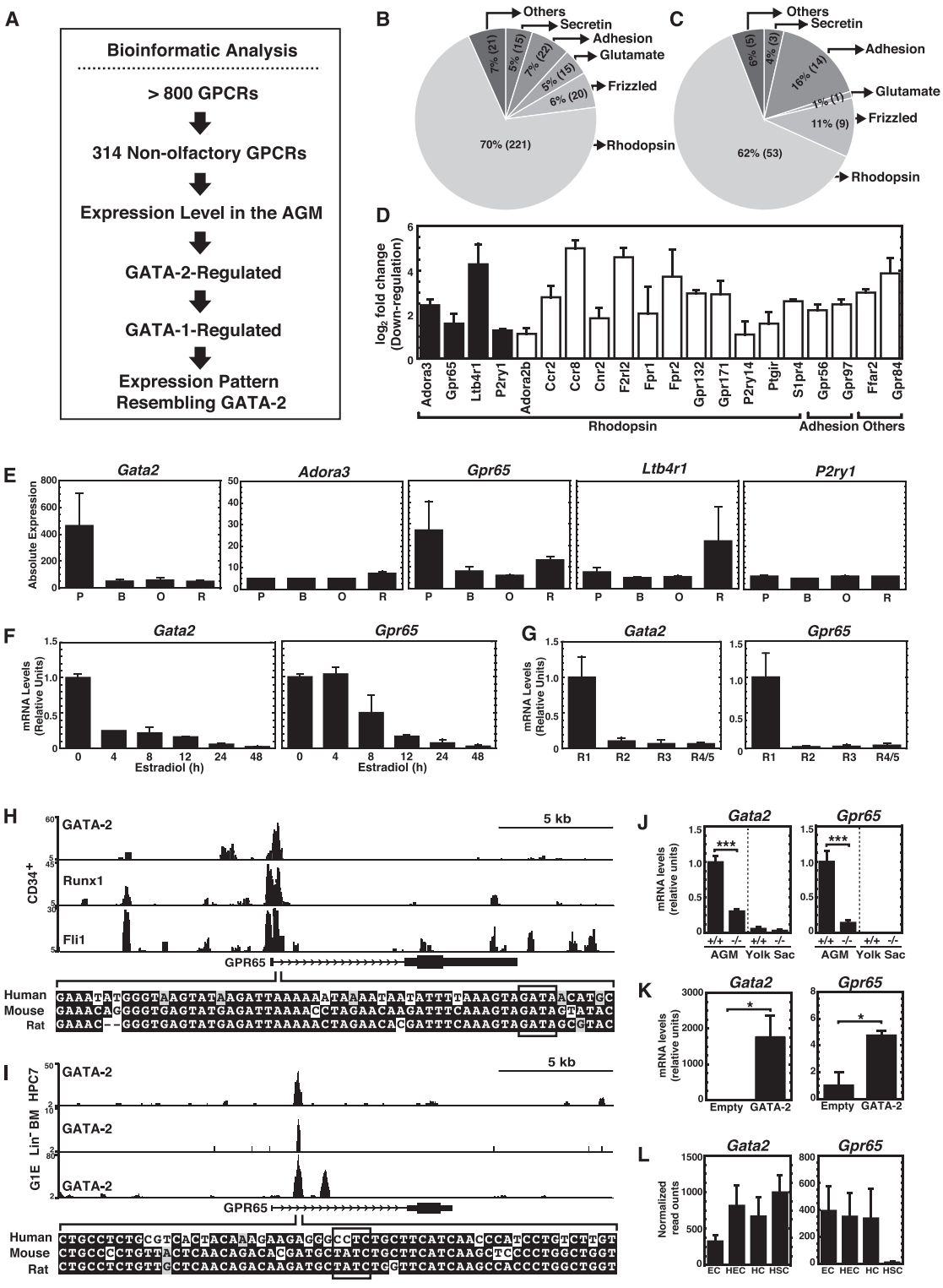

Figure 3. Global GPCR Analysis in the AGM

(A) Global GPCR analysis.

(B) Non-olfactory GPCRs (N = 314) were categorized into Secretin, Adhesion, Glutamate, Frizzled/Taste2, and Rhodopsin families based on sequence homology.

(legend continued on next page)

might downregulate key regulators of HSC generation/activity. After knocking down GPR65, we isolated infected $CD31^{+}$c-KIT^{-} endothelial cells that give rise to HSCs. Downregulating *Gpr65* mRNA by 60%–70% increased *Gata2* mRNA 2.9-fold ($p = 0.03$) and its downstream target *Runx1* mRNA 2.9-fold ($p = 0.04$) (Figure 5D). The knockdown elevated *Gata2* primary transcripts 3.9-fold ($p = 0.04$) (Figure 5E), indicating that GPR65 suppresses *Gata2* transcription.

To determine whether GPR65 regulates *Gata2* expression in zebrafish, we analyzed *Gata2* expression using ISH at 36 hr post-fertilization. Zebrafish have two *Gata2* homologs; *Gata2b* is enriched in hemogenic endothelium and regulates HSPC emergence (Butko et al., 2015). Whereas the majority of uninjected embryos exhibited broad staining in the AGM, there was no clear linear zone enriched in hemogenic endothelium. However, *Gpr65*_ATG MO-injected embryos exhibited the linear zone (Figure S4), suggesting that GPR65 suppresses *Gata2* expression in zebrafish embryos. Given that GATA-2 promotes HSC emergence in the AGM and regulates HSC activity (de Pater et al., 2013; Gao et al., 2013), we propose that GPR65 suppresses hematopoiesis by limiting *Gata2* expression and GATA-2 levels.

As *Gpr65* is expressed in AGM endothelium and HSPCs, we asked whether GPR65 represses *Gata2* expression in other contexts. Fetal liver hematopoietic precursors express *Gata2*, and as GATA-1 rises upon erythroid maturation, *Gata2* is repressed (McIver et al., 2014). We isolated Lin^{-} hematopoietic precursors from E14.5 fetal livers (McIver et al., 2014) and tested whether reducing *Gpr65* expression with the *Gpr65* shRNA retrovirus alters *Gata2* expression. Cells were expanded for 72 hr to increase HSPCs, while suppressing differentiation. Downregulating *Gpr65* increased the proerythroblast-enriched R2 population 1.9-fold ($p = 0.0002$) and reduced the R3 population (early and late basophilic erythroblasts) 1.6-fold ($p = 0.0003$) (Figure 6A). Increased R2 cells, concomitant with reduced R3 cells, suggests that GPR65 promotes erythroid maturation. Downregulating *Gpr65* mRNA by 70%–80%, which lowered GPR65 protein by 50%, increased *Gata2* mRNA and primary transcripts 2.4 ($p = 3.65 \times 10^{-6}$) and 2.8-fold ($p = 0.014$), respectively (Figures 6B and 6C). Western blot analysis of fetal liver cells revealed that reducing GPR65 expression upregulated GATA-2 (Figure 6D). Increased GATA-2 selectively elevated GATA-2 target gene expression (Figure 6E). To test whether increased *Gata2* expression reflected a change in cellularity, we used FACS to isolate the GATA-2-expressing R2 population and compared gene expression in control and knockdown R2 cells. *Gpr65* knockdown upregulated *Gata2* mRNA 2.3-fold ($p = 0.02$), primary transcript 4.8-fold ($p = 0.01$), GATA-2 protein, and GATA-2 target genes in FACS-sorted R2 cells (Figures 6F–6I). These results indicate that GPR65 represses *Gata2* in the AGM and fetal liver. Since GATA-1 needs to repress *Gata2* transcription early in erythroid maturation, upregulated *Gata2* expression caused by the *Gpr65* knockdown would be expected to increase immature R2 cells as observed (Figure 6A).

The +9.5 enhances *Gata2* expression in the AGM and fetal liver (Gao et al., 2013; Johnson et al., 2012; Sanalkumar et al., 2014). Deleting the +9.5 abrogated HSC generation in the AGM (Gao et al., 2013) and disrupted establishment of the HSPC compartment in the fetal liver (Johnson et al., 2012). To determine whether increased *Gata2* transcription upon *Gpr65* knockdown requires the +9.5, we isolated Lin^{-} HSPCs from E14.5 + $9.5^{+/-}$ fetal livers and infected cells with *Gpr65* shRNA retrovirus. After 72 hr of expansion culture, allele-specific primers were used to quantitate primary transcripts from wild-type and mutant 9.5 alleles in fetal liver cells and FACS-purified R2 cells (Figure 6J). *Gpr65* knockdown upregulated *Gata2* primary transcripts from the wild-type, but not the +9.5 mutant, allele (Figure 6J), demonstrating importance of the +9.5 for *Gata2* transcription.

(C) Classification of 85 GPCRs expressed in the AGM (>5 transcripts per million) into five families.
(D) Bar graph depicting GATA-2-regulated genes from RNA-seq analysis of $+9.5^{+/+}$ and $+9.5^{-/-}$ AGMs (Gao et al., 2013). Black bars, genes co-regulated by GATA-1 according to our prior microarray analysis of G1E-ER-GATA with or without β-estradiol treatment (DeVilbiss et al., 2013).
(E) *Gata2, Adora3, Gpr65, Ltb4r1,* and *P2ry1* expression during erythropoiesis. B, basophilic erythroblast; O, polyorthochromatic erythroblast; P, proerythroblast; R, reticulocyte (http://www.cbil.upenn.edu/ErythronDB/).
(F) Time course of *Gata2* and *Gpr65* expression following β-estradiol treatment in G1E-ER-GATA cells (n = 3 independent experiments).
(G) RT-PCR analysis of *Gata2* and *Gpr65* in FACS-sorted R1, R2, R3, and R4/5 populations from fetal liver (n = 3 independent experiments).
(H and I) ChIP signal map for *Gpr65* in human CD34 cells (H) (Beck et al., 2013), mouse HPC7 cells (Wilson et al., 2010), Lin^{-} bone marrow cells (Li et al., 2011), and G1E cells (Trompouki et al., 2011) (I).
(J and K) RT-PCR analysis of *Gata2* and *Gpr65* mRNA in $+9.5^{+/+}$ and $+9.5^{-/-}$ AGM (5 litters: $+9.5^{+/+}$ [n = 8 embryos]; $+9.5^{-/-}$ [n = 6 embryos]) and yolk sac (three litters: $+9.5^{+/+}$ [n = 7 embryos]; $+9.5^{-/-}$ [n = 5 embryos]) (J), and MAE cells expressing GATA-2 (K) (n = 3 independent experiments).
(L) RNA-seq of *Gata2* and *Gpr65* mRNA in FACS-sorted endothelial cells (EC), hemogenic endothelial cells (HEC), hematopoietic cells (HC), and hematopoietic stem cells (HSC) from the AGM (Solaimani Kartalaei et al., 2015).
Error bars represent SEM. *$p < 0.05$; ***$p < 0.001$ (two-tailed unpaired Student's t test).

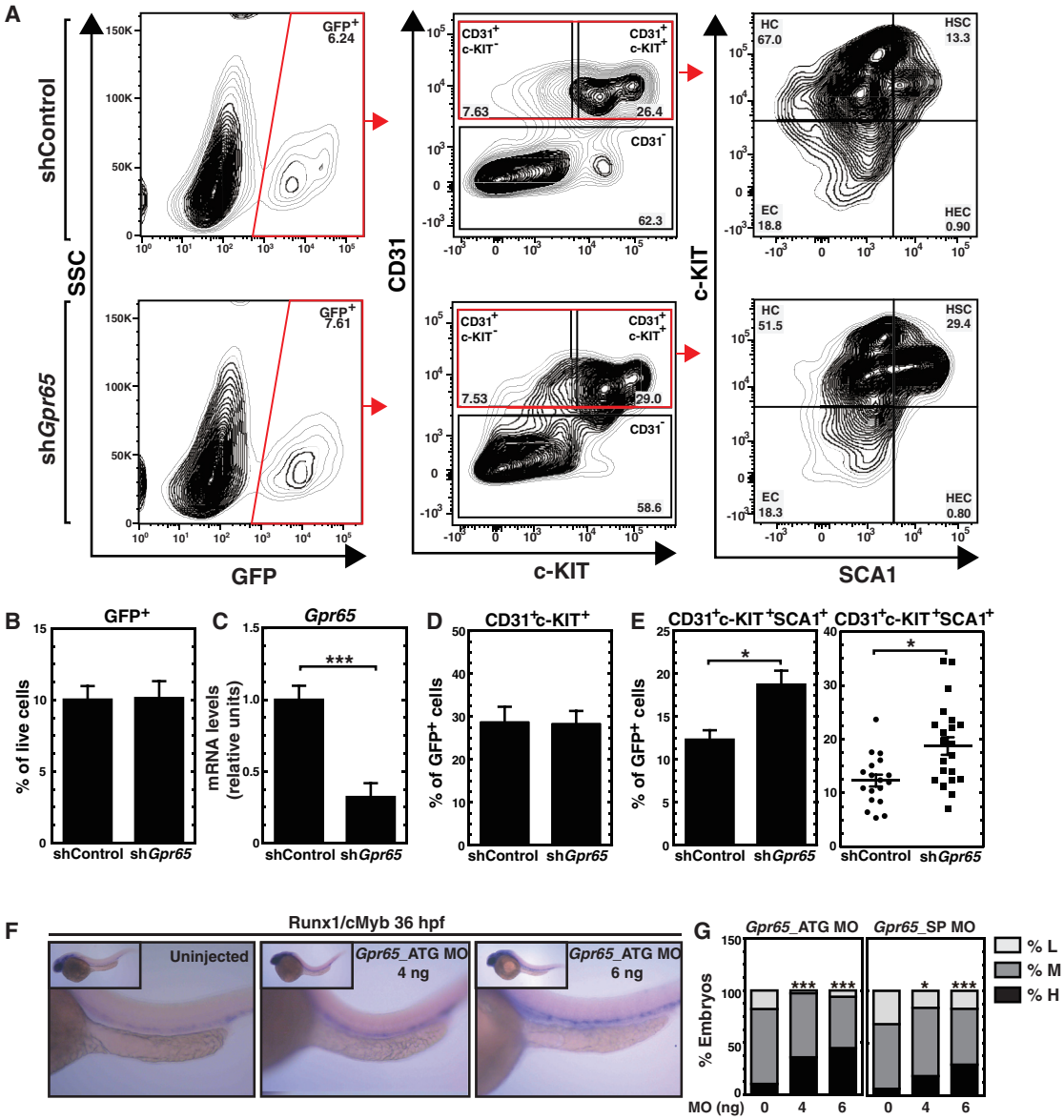

Figure 4. GPR65 Suppresses Hematopoiesis in the Mouse and Zebrafish AGM

(A) Representative flow cytometric plots of CD31$^+$c-KIT$^+$ and CD31$^+$c-KIT$^+$SCA1$^+$ cell populations in control or *Gpr65* shRNA-treated AGMs after 96 hr of culture.

(B) Quantitation of GFP$^+$ cells with total live cells (9 litters: shLuc [n = 22 embryos]; sh*Gpr65* [n = 26 embryos]).

(C) RT-PCR analysis of *Gpr65* mRNA levels in FACS-sorted GFP$^+$ cells (6 litters: shLuc [n = 15 embryos]; sh*Gpr65* [n = 15 embryos]).

(D and E) Analysis of flow cytometry data expressed as percentage of CD31$^+$c-KIT$^+$ (D) and CD31$^+$c-KIT$^+$Scal1$^+$ (E) cells in GFP$^+$ cells (D: 9 litters: shLuc [n = 22 embryos]; sh*Gpr65* [n = 26 embryos]; E: 7 litters: shLuc [n = 18]; sh*Gpr65* [n = 22]).

(F) Representative images of ISH with the HSPC markers *Runx1/cMyb* at 36 hr post-fertilization.

(G) Quantitation of ISH data expressed as percentage of embryos with high, medium, and low *Runx1/cMyb* staining in total embryos (ATG MO 0 ng [124 embryos]; ATG MO 4 ng [75 embryos]; ATG MO 6 ng [66 embryos]; SP MO 0 ng [97 embryos]; SP MO 4 ng [49 embryos]; SP MO 6 ng [58 embryos]). *Gpr65*_ATG MO: morpholino targeting the translation start site of *Gpr65*; *Gpr65*_SP MO: morpholino blocking the splicing of *Gpr65*.

Error bars represent SEM. *p < 0.05; ***p < 0.001 (two-tailed unpaired Student's t test).

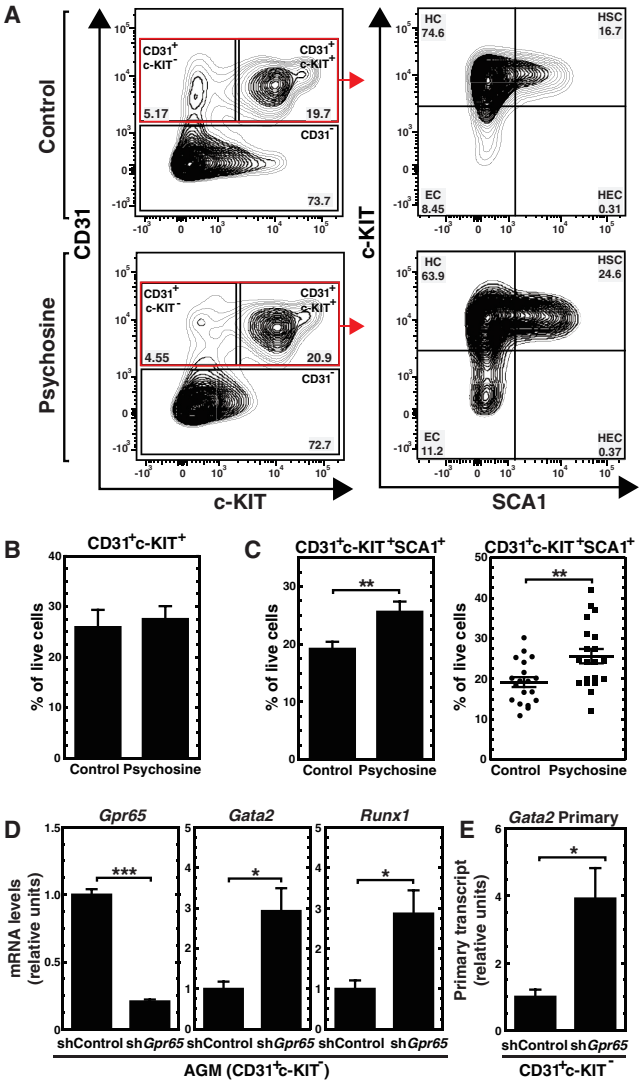

Figure 5. Psychosine Promotes Hematopoiesis in the AGM and GPR65 Suppresses Hematopoiesis by Repressing *Gata2* Expression

(A) Representative flow cytometric plots of $CD31^+c\text{-}KIT^+$ and $CD31^+c\text{-}KIT^+SCA1^+$ cell populations in the AGM after 4 days of culture with 20 μM psychosine.

(B and C) The average percentage of $CD31^+c\text{-}KIT^+$ (B) and $CD31^+c\text{-}KIT^+SCA1^+$ (C) cell populations with vehicle or psychosine treatment (6 litters: control [n = 19 embryos]; psychosine [n = 20 embryos]).

(D and E) RT-PCR analysis of *Gpr65*, *Gata2*, and *Runx1* mRNA (D) and *Gata2* primary transcript (E) in FACS-sorted $CD31^+c\text{-}KIT^-$ cells (n = 3 independent experiments).

Error bars represent SEM. *p < 0.05; **p < 0.01; ***p < 0.001 (two-tailed unpaired Student's t test).

Previously, we demonstrated that SetD8, the enzyme that monomethylates H4K20 (Beck et al., 2012), represses *Gata2* expression via the +9.5 site (DeVilbiss et al., 2015). We tested the relevance of this mechanism to GPR65-mediated *Gata2* repression. We conducted quantitative ChIP analysis for H4K20me1 in fetal liver cells (control or *Gpr65* knockdown) after culturing for 72 hr. Downregulating *Gpr65* did not alter the SetD8 mRNA level (Figure 6K). *Gpr65* downregulation reduced H4K20me1 at the +9.5 site (p = 0.002) and at sites 480 bp upstream (p = 0.002), 466 bp downstream (p = 0.006), and 880 bp downstream (p = 0.02) of the +9.5 site (Figure 6K). H4K20me1 was unaltered at the repressed muscle-specific *MyoD* promoter and the constitutively active *Eif3k* promoter. These results support a mechanism in which GPR65 represses *Gata2* by increasing a repressive chromatin mark at the +9.5 site. The basic helix-loop-helix transcription factor Scl/TAL1 activates *Gata2* transcription through the +9.5 site, and Scl1/TAL1 chromatin occupancy is reduced at the +9.5 site during GATA-1-mediated *Gata2* repression (Sanalkumar et al., 2014). As *Gpr65* downregulation decreased H4K20me1 at the +9.5 site, this alteration may generate chromatin that is more accessible to cognate binding factors. To determine whether GPR65 alters GATA-1 and Scl/TAL1 occupancy, we quantitated GATA-1 and Scl/TAL1 occupancy at the +9.5 site in fetal liver cells infected with control shRNA or *Gpr65* shRNA-expressing retrovirus. While knocking down *Gpr65* did not alter GATA-1 occupancy at the +9.5, the knockdown increased Scl/TAL1 occupancy at the +9.5 1.6-fold (p = 0.02) but not at other target loci (*Lyl1* and *Kit*) (Figures 6K and S5). These results suggest that GPR65 represses *Gata2* by establishing repressive chromatin that limits Scl/TAL1 occupancy at the +9.5 site (Figure 6L).

DISCUSSION

Genetic networks orchestrating stem and progenitor cell transitions can be deconstructed into regulatory modules termed network motifs (Alon, 2007; Shoval and Alon, 2010). Whereas major progress has been made to identify individual genes controlling hematopoiesis (Gao et al., 2013; Guo et al., 2013; Lara-Astiaso et al., 2014; Li et al., 2014; Moignard et al., 2013; Solaimani Kartalaei et al., 2015), many questions remain unanswered regarding how the genes form network motifs, how the network motifs amalgamate into circuitry, and whether the circuitry has an inherent plasticity and undergoes remodeling in states of altered hematopoiesis such as stress, aging, and malignancy.

Since the GATA-2-dependent genetic network promotes hematopoiesis (Gao et al., 2013; Solaimani Kartalaei et al., 2015), it is reasonable to infer that GATA-2-induced factors are positive mediators of key steps, including EHT, HSPC self-renewal, and differentiation. In erythroid cells, GATA-1 activates heme biosynthetic genes, globin

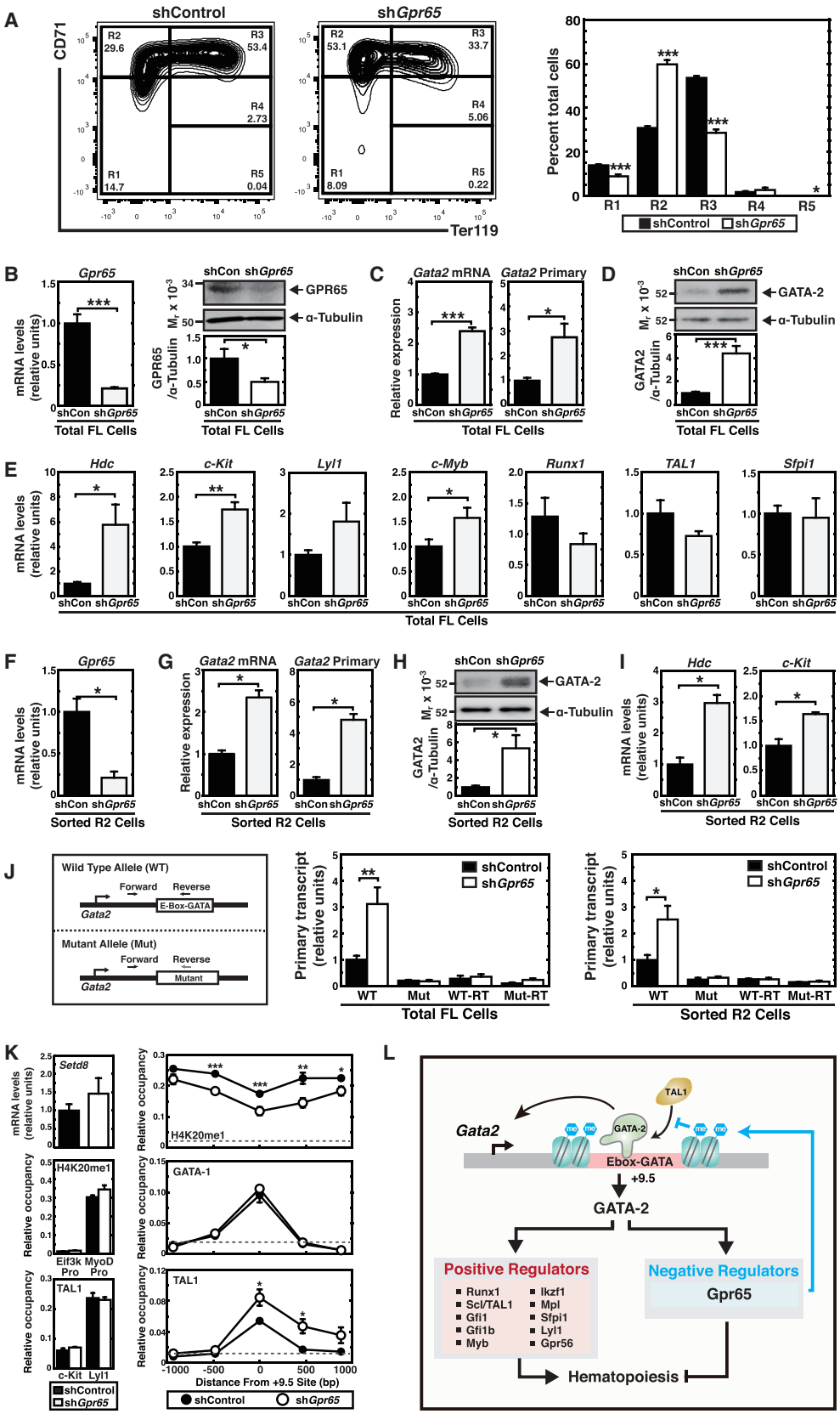

(legend on next page)

subunits, and constituents of the red cell cytoskeleton (Cheng et al., 2009; Fujiwara et al., 2009; Welch et al., 2004; Yu et al., 2009), all required for erythroid maturation. Moreover, GATA-1 represses *Gata2*, *Lyl1*, and *Kit* (Grass et al., 2003; Johnson et al., 2007; Munugalavadla et al., 2005), to enable erythroid maturation. GATA-2 activates *Kit* (Jing et al., 2008), an essential regulator of HSPCs (Heissig et al., 2002; Huang et al., 1990), consistent with GATA-2 promoting HSPC genesis and function.

Using a coupled bioinformatics-experimental strategy, we analyzed the large GPCR gene family to discover GATA-2-induced GPCRs that promote HSPC transitions. This analysis led to the surprising finding that GATA-2 activates *Gpr65* expression, which suppresses hematopoiesis via negative feedback on *Gata2*. This negative feedback mechanism conforms to a type I incoherent feedforward loop (Mangan and Alon, 2003), which is defined as an input (GATA-2) that elicits an output (EHT or hematopoiesis) through positive (increased *Gpr65* expression) and negative (GPR65 suppression of hematopoiesis) paths. Type I incoherent feedforward loops shape the dynamics of a mechanism, with the feedforward loop conferring a pulse of activity to accelerate the reaction (Mangan and Alon, 2003). Since the constituents and network motifs governing HSPC transitions are still being identified, the dynamics of steps in these transitions are largely unexplored. The mechanism of GPR65-mediated *Gata2* repression involved elevation of a repressive histone mark, H4K20me1, linked to reduced occupancy by the activator Scl/TAL1. GPR65 might directly target chromatin to restrict Scl/TAL1 occupancy or might reduce Scl/TAL1 occupancy prior to chromatin modification. Regardless of the order of events, our analysis established a GATA factor-GPCR-dependent type I incoherent feedforward loop that suppresses, rather than promotes hematopoiesis.

Gpr65, or T cell death-associated gene 8 (*Tdag8*), is a proton/acid-activated GPCR (Choi et al., 1996; Wang et al., 2004). Whereas GPR65 had not been linked to HSPC transitions, it was reported to be a pro-apoptotic factor in glucocorticoid-induced lymphocyte apoptosis (Malone et al., 2004) and to regulate cytokine production from macrophages (Mogi et al., 2009). Targeted deletion of *Gpr65* revealed it was dispensable for glucocorticoid-induced thymocyte apoptosis (Radu et al., 2006). These results were suggested to reflect redundancy with related pH-sensing GPCRs, which would create an obstacle to dissect *Gpr65* function in vivo. Although the impact of the pH-sensing mechanism to GATA-2 function in the AGM and fetal liver is unclear, the endogenous GPR65 antagonist psychosine resembled *Gpr65* shRNA in upregulating *Gata2* expression and hematopoiesis.

As GPR65 suppressed HSPC generation from mouse AGM explants, it is instructive to consider the consequences of ablating this mechanism in vivo. Abrogation of the mechanism would promote HSPC genesis and function. Since ablating *Gpr65* would be expected to increase HSPCs,

Figure 6. GPR65 Enhances H4K20me1 and Limits Scl/TAL1 Occupancy at the +9.5 Enhancer

(A) Representative flow cytometric plots of erythroid maturation based on CD71 and Ter119 expression 3 days after HSPC expansion. The average percentage of cells in R1 through R5 populations after infection with control or *Gpr65* shRNA is depicted on the right (n = 3 independent experiments).

(B) RT-PCR analysis of *Gpr65* mRNA in fetal liver cells (n = 5 independent experiments) (left). Western blot of GPR65 in fetal liver cells (top right), and quantification of GPR65 and α-tubulin intensities by densitometry (n = 8 independent experiments) (bottom right).

(C) RT-PCR analysis of *Gata2* mRNA and primary transcript in total fetal liver cells (n = 5 independent experiments).

(D) Western blot of GATA-2 in fetal liver cells (top) and quantification of GATA-2/α-tubulin ratio by densitometry (n = 6 independent experiments) (bottom).

(E) RT-PCR analysis of GATA-2 target gene expression in fetal liver cells (n = 5 independent experiments).

(F–I) Real-time RT-PCR analysis of *Gpr65* mRNA (F), *Gata2* mRNA (G), *Gata2* primary transcript (G), and GATA-2 target genes in FACS-sorted R2 cells (n = 3 independent experiments) (I). Western blot of GATA-2 in FACS-sorted R2 cells and quantification of intensities of GATA-2 to α-tubulin band by densitometric analysis (n = 4 independent experiments) (H).

(J) Fetal liver HSPCs were isolated from E14.5 embryos heterozygous for the +9.5 site at *Gata2*. Cells were infected with control or sh*Gpr65* and expanded for 3 days (left). Allele-specific real-time RT-PCR analysis of *Gata2* transcripts from the wild-type and mutant +9.5 alleles in total fetal liver cells (n = 3 independent experiments) (middle) and FACS-sorted R2 cells (n = 3 independent experiments) (right).

(K) RT-PCR analysis of *Setd8* mRNA in fetal liver cells treated with control or *Gpr65* shRNA (n = 5 independent experiments) (top left). H4K20me1, GATA-1, and Scl/TAL1 chromatin occupancy measured by quantitative ChIP at the +9.5 site in expanding fetal liver HSPCs treated with control or *Gpr65* shRNA (H4K20me1: n = 8 independent experiments; GATA-1: n = 4 independent experiments; Scl/TAL1: n = 6 independent experiments) (right). H4K20me1 levels at the repressed MyoD promoter and the active *Eif3k* promoter (middle left). Scl/TAL1 chromatin occupancy 114 kb upstream from the *c-Kit* promoter and Lyl1 exon1 as controls (bottom left). The dashed line illustrates the highest value obtained with PI antibody.

(L) GATA-2, a positive regulator of hematopoiesis, upregulates *Gpr65,* which encodes a negative regulator of hematopoiesis, to control HSC emergence. GPR65 represses *Gata2* expression by increasing H4K20me1, which restricts +9.5 occupancy by the activator Scl/TAL1.

Error bars represent SEM. *p < 0.05; **p < 0.01; ***p < 0.001 (two-tailed unpaired Student's t test).

evaluating the role of the GATA-2-GPR65 circuit in vivo will require a careful quantitative analysis. Considerations of type I incoherent feedforward loops (Alon, 2007; Mangan and Alon, 2003) would infer an alteration of the dynamics of specific steps of hematopoiesis, which might not be evident from steady-state analyses. It is attractive to propose that this suppressive mechanism is vital when the demand for hematopoiesis increases, e.g. during stress, since an unopposed increase could yield deleterious blood cell elevations.

In summary, we discovered that GATA-2 activity to promote hematopoiesis involves induction of both positive and negative mediators, the balance of which establishes the physiological output. Based on the GPR65 pH-sensing function, it will be crucial to analyze the pH microenvironment of the AGM and other sites of hematopoiesis and to establish the role of GPR65 as a mediator of pH-dependent HSPC transitions.

EXPERIMENTAL PROCEDURES

Mice and Embryo Generation

Gata2 +9.5-mutant mice were described by Johnson et al. (2012). Pregnant females were euthanized with CO_2, and freshly isolated embryos were transferred into cold PBS for dissection. Animal experiments were carried out with ethical approval of the Association for the Assessment and Accreditation of Laboratory Animal Care at the University of Wisconsin-Madison.

AGM Explant Culture

AGMs were dissected from E11.5 embryos. AGMs were infected (see below) and cultured as described by Gao et al. (2013). Intact AGMs were cultured for 4 days on Durapore filters (Millipore) at the air-liquid interface in IMDM$^+$ (Iscove's modified Dulbecco's medium) (Gibco) supplemented with 20% fetal bovine serum (FBS; Gemini), 4 mM L-glutamine (Gibco), 1% penicillin/streptomycin (Cellgro), 0.1 mM mercaptoethanol, 100 ng/ml interleukin-3 (R&D Systems), 100 ng/ml Flt3L (R&D), and 1.5% conditioned medium from a Kit ligand-producing Chinese hamster ovary cell line.

Retroviral Infection

Detailed methodology is presented in Supplemental Experimental Procedures. *Gpr65* shRNA were cloned into the MSCV-PIG (IRES-GFP) vector (kindly provided by Dr. Mitchell Weiss) (McIver et al., 2014) using BglII and XhoI restriction sites. Retroviral expression vectors for *Gata2* and shLuc were described by Katsumura et al. (2014). Retroviruses were packaged by co-transfecting 293T cells with pCL-Eco packaging vector. Retroviral supernatant was collected 24 and 48 hr post transfection and centrifuged to remove cells and debris. The Retro-X Concentrator (Clontech #631455) was used to concentrate retrovirus. E11.5 AGMs were infected with 20 μl concentrated retrovirus and 8 μg/ml polybrene in 500 μl explant culture media at 1,200 × *g* for 90 min at 30°C. AGMs were subjected to explant culture. Primary erythroid precursors were spinfected with 100 μl retrovirus supernatant and 8 μg/ml polybrene in 400 μl fetal liver expansion medium at 1,200 × *g* for 90 min at 30°C. After centrifugation, 500 μl pre-warmed fetal liver expansion medium was added, and cells were incubated at 37°C for 72 hr. Details for concentrating retrovirus and *Gpr65* shRNA sequences are available in Supplemental Experimental Procedures.

Flow Cytometry

Detailed methodology is presented in Supplemental Experimental Procedures.

ChIP Assay

Detailed methodology is presented in Supplemental Experimental Procedures.

Zebrafish Morpholino Knockdown

Detailed methodology is presented in Supplemental Experimental Procedures.

Statistical Analysis

Student's t tests were conducted using GraphPad Software or Microsoft Excel. p Values in all figures are denoted by asterisks: *$p < 0.05$, **$p < .01$, and ***$p < .001$.

ACCESSION NUMBERS

The accession number for GATA-2, RUNX1, and FLI1 ChIP-seq in human CD34$^+$ cells reported in the paper is GEO: GSE45144. The accession number for GATA-2 and TAL1 ChIP-seq in HPC7 cells reported in the paper is GEO: GSE22178. The accession number for GATA-2 ChIP-seq in Lin$^-$ BM cells reported in the paper is GEO: GSM641911. The accession number for GATA-2 ChIP-seq in G1E cells reported in the paper is GEO: GSM722387.

SUPPLEMENTAL INFORMATION

Supplemental Information includes Supplemental Experimental Procedures and five figures and can be found with this article online at http://dx.doi.org/10.1016/j.stemcr.2016.01.008.

AUTHOR CONTRIBUTIONS

All authors participated in designing experiments and/or analyzing data. J.L.L. conducted the zebrafish experiments and analyzed the data. X.G. and E.H.B. wrote the manuscript in consultation with other authors.

ACKNOWLEDGMENTS

The work was supported by NIH DK68634 and DK50107 (to E.H.B.), Cancer Center Support Grant P30CA014520, and NIH HL04880, HL032262, HL10001-05, and DK092760 (to L.I.Z). We thank Michelle Ammerman and Prathibha Sanalkumar for assistance with zebrafish experiments and Western blotting, respectively.

Received: September 13, 2015
Revised: January 11, 2016
Accepted: January 13, 2016
Published: February 18, 2016

REFERENCES

Adams, G.B., Alley, I.R., Chung, U.I., Chabner, K.T., Jeanson, N.T., Lo Celso, C., Marsters, E.S., Chen, M., Weinstein, L.S., Lin, C.P., et al. (2009). Haematopoietic stem cells depend on Galpha(s)-mediated signalling to engraft bone marrow. Nature *459*, 103–107.

Alon, U. (2007). Network motifs: theory and experimental approaches. Nat. Rev. Genet. *8*, 450–461.

Beck, D.B., Oda, H., Shen, S.S., and Reinberg, D. (2012). PR-Set7 and H4K20me1: at the crossroads of genome integrity, cell cycle, chromosome condensation, and transcription. Genes Dev. *26*, 325–337.

Beck, D., Thoms, J.A., Perera, D., Schutte, J., Unnikrishnan, A., Knezevic, K., Kinston, S.J., Wilson, N.K., O'Brien, T.A., Gottgens, B., et al. (2013). Genome-wide analysis of transcriptional regulators in human HSPCs reveals a densely interconnected network of coding and noncoding genes. Blood *122*, e12–22.

Bertrand, J.Y., Chi, N.C., Santoso, B., Teng, S., Stainier, D.Y., and Traver, D. (2010). Haematopoietic stem cells derive directly from aortic endothelium during development. Nature *464*, 108–111.

Boisset, J.C., van Cappellen, W., Andrieu-Soler, C., Galjart, N., Dzierzak, E., and Robin, C. (2010). In vivo imaging of haematopoietic cells emerging from the mouse aortic endothelium. Nature *464*, 116–120.

Broxmeyer, H.E., Orschell, C.M., Clapp, D.W., Hangoc, G., Cooper, S., Plett, P.A., Liles, W.C., Li, X., Graham-Evans, B., Campbell, T.B., et al. (2005). Rapid mobilization of murine and human hematopoietic stem and progenitor cells with AMD3100, a CXCR4 antagonist. J. Exp. Med. *201*, 1307–1318.

Butko, E., Distel, M., Pouget, C., Weijts, B., Kobayashi, I., Ng, K., Mosimann, C., Poulain, F.E., McPherson, A., Ni, C.W., et al. (2015). Gata2b is a restricted early regulator of hemogenic endothelium in the zebrafish embryo. Development *142*, 1050–1061.

Cheng, Y., Wu, W., Kumar, S.A., Yu, D., Deng, W., Tripic, T., King, D.C., Chen, K.-B., Zhang, Y., Drautz, D., et al. (2009). Erythroid GATA1 function revealed by genome-wide analysis of transcription factor occupancy, histone modifications, and mRNA expression. Genome Res. *19*, 2172–2184.

Choi, J.W., Lee, S.Y., and Choi, Y. (1996). Identification of a putative G protein-coupled receptor induced during activation-induced apoptosis of T cells. Cell Immunol. *168*, 78–84.

de Pater, E., Kaimakis, P., Vink, C.S., Yokomizo, T., Yamada-Inagawa, T., van der Linden, R., Kartalaei, P.S., Camper, S.A., Speck, N., and Dzierzak, E. (2013). Gata2 is required for HSC generation and survival. J. Exp. Med. *210*, 2843–2850.

DeVilbiss, A.W., Boyer, M.E., and Bresnick, E.H. (2013). Establishing a hematopoietic genetic network through locus-specific integration of chromatin regulators. Proc. Natl. Acad. Sci. USA *110*, E3398–E3407.

DeVilbiss, A.W., Sanalkumar, R., Hall, B.D., Katsumura, K.R., de Andrade, I.F., and Bresnick, E.H. (2015). Epigenetic determinants of erythropoiesis: role of the histone methyltransferase SetD8 in promoting erythroid cell maturation and survival. Mol. Cell Biol. *35*, 2073–2087.

Dzierzak, E., and Speck, N.A. (2008). Of lineage and legacy: the development of mammalian hematopoietic stem cells. Nat. Immunol. *9*, 129–136.

Fujiwara, T., O'Geen, H., Keles, S., Blahnik, K., Linnemann, A.K., Kang, Y.A., Choi, K., Farnham, P.J., and Bresnick, E.H. (2009). Discovering hematopoietic mechanisms through genome-wide analysis of GATA factor chromatin occupancy. Mol. Cell *36*, 667–681.

Gao, X., Johnson, K.D., Chang, Y.I., Boyer, M.E., Dewey, C.N., Zhang, J., and Bresnick, E.H. (2013). Gata2 cis-element is required for hematopoietic stem cell generation in the mammalian embryo. J. Exp. Med. *210*, 2833–2842.

Goessling, W., Allen, R.S., Guan, X., Jin, P., Uchida, N., Dovey, M., Harris, J.M., Metzger, M.E., Bonifacino, A.C., Stroncek, D., et al. (2011). Prostaglandin E2 enhances human cord blood stem cell xenotransplants and shows long-term safety in preclinical nonhuman primate transplant models. Cell Stem Cell *8*, 445–458.

Grass, J.A., Boyer, M.E., Pal, S., Wu, J., Weiss, M.J., and Bresnick, E.H. (2003). GATA-1-dependent transcriptional repression of GATA-2 via disruption of positive autoregulation and domain-wide chromatin remodeling. Proc. Natl. Acad. Sci. USA *100*, 8811–8816.

Grass, J.A., Jing, H., Kim, S.-I., Martowicz, M.L., Pal, S., Blobel, G.A., and Bresnick, E.H. (2006). Distinct functions of dispersed GATA factor complexes at an endogenous gene locus. Mol. Cell Biol. *26*, 7056–7067.

Guiu, J., Shimizu, R., D'Altri, T., Fraser, S.T., Hatakeyama, J., Bresnick, E.H., Kageyama, R., Dzierzak, E., Yamamoto, M., Espinosa, L., et al. (2013). Hes repressors are essential regulators of hematopoietic stem cell development downstream of Notch signaling. J. Exp. Med. *210*, 71–84.

Guo, G., Luc, S., Marco, E., Lin, T.W., Peng, C., Kerenyi, M.A., Beyaz, S., Kim, W., Xu, J., Das, P.P., et al. (2013). Mapping cellular hierarchy by single-cell analysis of the cell surface repertoire. Cell Stem Cell *13*, 492–505.

Heissig, B., Hattori, K., Dias, S., Friedrich, M., Ferris, B., Hackett, N.R., Crystal, R.G., Besmer, P., Lyden, D., Moore, M.A., et al. (2002). Recruitment of stem and progenitor cells from the bone marrow niche requires MMP-9 mediated release of kit-ligand. Cell *109*, 625–637.

Hoggatt, J., Mohammad, K.S., Singh, P., Hoggatt, A.F., Chitteti, B.R., Speth, J.M., Hu, P., Poteat, B.A., Stilger, K.N., Ferraro, F., et al. (2013). Differential stem- and progenitor-cell trafficking by prostaglandin E2. Nature *495*, 365–369.

Hsu, A.P., Johnson, K.D., Falcone, E.L., Sanalkumar, R., Sanchez, L., Hickstein, D.D., Cuellar-Rodriguez, J., Lemieux, J.E., Zerbe, C.S., Bresnick, E.H., et al. (2013). GATA2 haploinsufficiency caused by mutations in a conserved intronic element leads to MonoMAC syndrome. Blood *121*, 3830–3837, S1–7.

Huang, E., Nocka, K., Beier, D.R., Chu, T.Y., Buck, J., Lahm, H.W., Wellner, D., Leder, P., and Besmer, P. (1990). The hematopoietic growth factor KL is encoded by the Sl locus and is the ligand of the c-kit receptor, the gene product of the W locus. Cell *63*, 225–233.

Im, D.S., Heise, C.E., Nguyen, T., O'Dowd, B.F., and Lynch, K.R. (2001). Identification of a molecular target of psychosine and its role in globoid cell formation. J. Cell Biol. *153*, 429–434.

Jing, H., Vakoc, C.R., Ying, L., Mandat, S., Wang, H., Zheng, X., and Blobel, G.A. (2008). Exchange of GATA factors mediates transitions in looped chromatin organization at a developmentally regulated gene locus. Mol. Cell *29*, 232–242.

Johnson, K.D., Boyer, M.E., Kang, J.A., Wickrema, A., Cantor, A.B., and Bresnick, E.H. (2007). Friend of GATA-1-independent transcriptional repression: a novel mode of GATA-1 function. Blood *109*, 5230–5233.

Johnson, K.D., Hsu, A.P., Ryu, M.J., Wang, J., Gao, X., Boyer, M.E., Liu, Y., Lee, Y., Calvo, K.R., Keles, S., et al. (2012). Cis-element mutated in GATA2-dependent immunodeficiency governs hematopoiesis and vascular integrity. J. Clin. Invest. *122*, 3692–3704.

Johnson, K.D., Kong, G., Gao, X., Chang, Y.-I., Hewitt, K.J., Sanalkumar, R., Prathibha, R., Ranheim, E.A., Dewey, C.N., Zhang, J., et al. (2015). Cis-regulatory mechanisms governing stem and progenitor cell transitions. Sci. Adv. *1*, e1500503.

Katsumura, K.R., Yang, C., Boyer, M.E., Li, L., and Bresnick, E.H. (2014). Molecular basis of crosstalk between oncogenic Ras and the master regulator of hematopoiesis GATA-2. EMBO Rep. *15*, 938–947.

Kingsley, P.D., Greenfest-Allen, E., Frame, J.M., Bushnell, T.P., Malik, J., McGrath, K.E., Stoeckert, C.J., and Palis, J. (2013). Ontogeny of erythroid gene expression. Blood *121*, e5–e13.

Lagerstrom, M.C., and Schioth, H.B. (2008). Structural diversity of G protein-coupled receptors and significance for drug discovery. Nat. Rev. Drug Discov. *7*, 339–357.

Lara-Astiaso, D., Weiner, A., Lorenzo-Vivas, E., Zaretsky, I., Jaitin, D.A., David, E., Keren-Shaul, H., Mildner, A., Winter, D., Jung, S., et al. (2014). Immunogenetics. Chromatin state dynamics during blood formation. Science *345*, 943–949.

Li, L., Jothi, R., Cui, K., Lee, J.Y., Cohen, T., Gorivodsky, M., Tzchori, I., Zhao, Y., Hayes, S.M., Bresnick, E.H., et al. (2011). Nuclear adaptor Ldb1 regulates a transcriptional program essential for the maintenance of hematopoietic stem cells. Nat. Immunol. *12*, 129–136.

Li, Y., Esain, V., Teng, L., Xu, J., Kwan, W., Frost, I.M., Yzaguirre, A.D., Cai, X., Cortes, M., Maijenburg, M.W., et al. (2014). Inflammatory signaling regulates embryonic hematopoietic stem and progenitor cell production. Genes Dev. *28*, 2597–2612.

Li, C., Lan, Y., Schwartz-Orbach, L., Korol, E., Tahiliani, M., Evans, T., and Goll, M.G. (2015). Overlapping requirements for Tet2 and Tet3 in Normal development and hematopoietic stem cell emergence. Cell Rep. *12*, 1133–1143.

Ling, K.W., Ottersbach, K., van Hamburg, J.P., Oziemlak, A., Tsai, F.Y., Orkin, S.H., Ploemacher, R., Hendriks, R.W., and Dzierzak, E. (2004). GATA-2 plays two functionally distinct roles during the ontogeny of hematopoietic stem cells. J. Exp. Med. *200*, 871–882.

Liu, F., Li, D., Yu, Y.Y., Kang, I., Cha, M.J., Kim, J.Y., Park, C., Watson, D.K., Wang, T., and Choi, K. (2015). Induction of hematopoietic and endothelial cell program orchestrated by ETS transcription factor ER71/ETV2. EMBO Rep. *16*, 654–669.

Lugus, J.J., Chung, Y.S., Mills, J.C., Kim, S.I., Grass, J., Kyba, M., Doherty, J.M., Bresnick, E.H., and Choi, K. (2007). GATA2 functions at multiple steps in hemangioblast development and differentiation. Development *134*, 393–405.

Maeno, M., Mead, P.E., Kelley, C., Xu, R.H., Kung, H.F., Suzuki, A., Ueno, N., and Zon, L.I. (1996). The role of BMP-4 and GATA-2 in the induction and differentiation of hematopoietic mesoderm in Xenopus laevis. Blood *88*, 1966–1972.

Malone, M.H., Wang, Z., and Distelhorst, C.W. (2004). The glucocorticoid-induced gene tdag8 encodes a pro-apoptotic G protein-coupled receptor whose activation promotes glucocorticoid-induced apoptosis. J. Biol. Chem. *279*, 52850–52859.

Mangan, S., and Alon, U. (2003). Structure and function of the feed-forward loop network motif. Proc. Natl. Acad. Sci. USA *100*, 11980–11985.

May, G., Soneji, S., Tipping, A.J., Teles, J., McGowan, S.J., Wu, M., Guo, Y., Fugazza, C., Brown, J., Karlsson, G., et al. (2013). Dynamic analysis of gene expression and genome-wide transcription factor binding during lineage specification of multipotent progenitors. Cell Stem Cell *13*, 754–768.

McIver, S.C., Kang, Y.A., DeVilbiss, A.W., O'Driscoll, C.A., Ouellette, J.N., Pope, N.J., Camprecios, G., Chang, C.J., Yang, D., Bouhassira, E.E., et al. (2014). The exosome complex establishes a barricade to erythroid maturation. Blood *124*, 2285–2297.

Mogi, C., Tobo, M., Tomura, H., Murata, N., He, X.D., Sato, K., Kimura, T., Ishizuka, T., Sasaki, T., Sato, T., et al. (2009). Involvement of proton-sensing TDAG8 in extracellular acidification-induced inhibition of proinflammatory cytokine production in peritoneal macrophages. J. Immunol. *182*, 3243–3251.

Moignard, V., Macaulay, I.C., Swiers, G., Buettner, F., Schutte, J., Calero-Nieto, F.J., Kinston, S., Joshi, A., Hannah, R., Theis, F.J., et al. (2013). Characterization of transcriptional networks in blood stem and progenitor cells using high-throughput single-cell gene expression analysis. Nat. Cell Biol. *15*, 363–372.

Munugalavadla, V., Dore, L.C., Tan, B.L., Hong, L., Vishnu, M., Weiss, M.J., and Kapur, R. (2005). Repression of c-kit and its downstream substrates by GATA-1 inhibits cell proliferation during erythroid maturation. Mol. Cell Biol. *25*, 6747–6759.

North, T.E., Goessling, W., Walkley, C.R., Lengerke, C., Kopani, K.R., Lord, A.M., Weber, G.J., Bowman, T.V., Jang, I.H., Grosser, T., et al. (2007). Prostaglandin E2 regulates vertebrate haematopoietic stem cell homeostasis. Nature *447*, 1007–1011.

Orkin, S.H., and Zon, L.I. (2008). Hematopoiesis: an evolving paradigm for stem cell biology. Cell *132*, 631–644.

Radu, C.G., Nijagal, A., McLaughlin, J., Wang, L., and Witte, O.N. (2005). Differential proton sensitivity of related G protein-coupled receptors T cell death-associated gene 8 and G2A expressed in immune cells. Proc. Natl. Acad. Sci. USA *102*, 1632–1637.

Radu, C.G., Cheng, D., Nijagal, A., Riedinger, M., McLaughlin, J., Yang, L.V., Johnson, J., and Witte, O.N. (2006). Normal immune development and glucocorticoid-induced thymocyte apoptosis in mice deficient for the T-cell death-associated gene 8 receptor. Mol. Cell Biol. *26*, 668–677.

Robert-Moreno, A., Guiu, J., Ruiz-Herguido, C., Lopez, M.E., Ingles-Esteve, J., Riera, L., Tipping, A., Enver, T., Dzierzak, E., Gridley, T.,

et al. (2008). Impaired embryonic haematopoiesis yet normal arterial development in the absence of the Notch ligand Jagged1. EMBO J. *27*, 1886–1895.

Rodrigues, N.P., Janzen, V., Forkert, R., Dombkowski, D.M., Boyd, A.S., Orkin, S.H., Enver, T., Vyas, P., and Scadden, D.T. (2005). Haploinsufficiency of GATA-2 perturbs adult hematopoietic stem cell homeostasis. Blood *106*, 477–484.

Roth, B.L., and Kroeze, W.K. (2015). Integrated approaches for genome-wide interrogation of the druggable non-olfactory g protein-coupled receptor superfamily. J. Biol. Chem. *290*, 19471–19477.

Saito, Y., Kaneda, K., Suekane, A., Ichihara, E., Nakahata, S., Yamakawa, N., Nagai, K., Mizuno, N., Kogawa, K., Miura, I., et al. (2013). Maintenance of the hematopoietic stem cell pool in bone marrow niches by EVI1-regulated GPR56. Leukemia *27*, 1637–1649.

Sanalkumar, R., Johnson, K.D., Gao, X., Boyer, M.E., Chang, Y.I., Hewitt, K.J., Zhang, J., and Bresnick, E.H. (2014). Mechanism governing a stem cell-generating cis-regulatory element. Proc. Natl. Acad. Sci. USA *111*, E1091–E1100.

Shoval, O., and Alon, U. (2010). SnapShot: network motifs. Cell *143*, 326-e1.

Solaimani Kartalaei, P., Yamada-Inagawa, T., Vink, C.S., de Pater, E., van der Linden, R., Marks-Bluth, J., van der Sloot, A., van den Hout, M., Yokomizo, T., van Schaick-Solerno, M.L., et al. (2015). Whole-transcriptome analysis of endothelial to hematopoietic stem cell transition reveals a requirement for Gpr56 in HSC generation. J. Exp. Med. *212*, 93–106.

Sugimoto, Y., and Narumiya, S. (2007). Prostaglandin E receptors. J. Biol. Chem. *282*, 11613–11617.

Tobo, A., Tobo, M., Nakakura, T., Ebara, M., Tomura, H., Mogi, C., Im, D.S., Murata, N., Kuwabara, A., Ito, S., et al. (2015). Characterization of imidazopyridine compounds as negative allosteric modulators of proton-sensing GPR4 in extracellular acidification-induced responses. PLoS One *10*, e0129334.

Tripic, T., Deng, W., Cheng, Y., Vakoc, C.R., Gregory, G.D., Hardison, R.C., and Blobel, G.A. (2008). SCL and associated protein distinguish active from repressive GATA transcription factor complexes. Blood *113*, 2191–2201.

Trompouki, E., Bowman, T.V., Lawton, L.N., Fan, Z.P., Wu, D.C., DiBiase, A., Martin, C.S., Cech, J.N., Sessa, A.K., Leblanc, J.L., et al. (2011). Lineage regulators direct BMP and Wnt pathways to cell specific programs during differentiation and regeneration. Cell *147*, 577–589.

Tsai, F.Y., Keller, G., Kuo, F.C., Weiss, M., Chen, J., Rosenblatt, M., Alt, F.W., and Orkin, S.H. (1994). An early haematopoietic defect in mice lacking the transcription factor GATA-2. Nature *371*, 221–226.

Wang, J.Q., Kon, J., Mogi, C., Tobo, M., Damirin, A., Sato, K., Komachi, M., Malchinkhuu, E., Murata, N., Kimura, T., et al. (2004). TDAG8 is a proton-sensing and psychosine-sensitive G-protein-coupled receptor. J. Biol. Chem. *279*, 45626–45633.

Welch, J.J., Watts, J.A., Vakoc, C.R., Yao, Y., Wang, H., Hardison, R.C., Blobel, G.A., Chodosh, L.A., and Weiss, M.J. (2004). Global regulation of erythroid gene expression by transcription factor GATA-1. Blood *104*, 3136–3147.

Wilson, N.K., Foster, S.D., Wang, X., Knezevic, K., Schutte, J., Kaimakis, P., Chilarska, P.M., Kinston, S., Ouwehand, W.H., Dzierzak, E., et al. (2010). Combinatorial transcriptional control in blood stem/progenitor cells: genome-wide analysis of ten major transcriptional regulators. Cell Stem Cell *7*, 532–544.

Wozniak, R.J., Keles, S., Lugus, J.J., Young, K., Boyer, M.E., Tran, T.T., Choi, K., and Bresnick, E.H. (2008). Molecular hallmarks of endogenous chromatin complexes containing master regulators of hematopoiesis. Mol. Cell Biol. *28*, 6681–6694.

Yu, M., Riva, L., Xie, H., Schindler, Y., Moran, T.B., Cheng, Y., Yu, D., Hardison, R., Weiss, M.J., Orkin, S.H., et al. (2009). Insights into GATA-1-mediated gene activation versus repression via genome-wide chromatin occupancy analysis. Mol. Cell *36*, 682–695.

Stem Cell Reports, Volume *6*

Supplemental Information

GATA Factor-G-Protein-Coupled Receptor Circuit Suppresses Hematopoiesis

Xin Gao, Tongyu Wu, Kirby D. Johnson, Jamie L. Lahvic, Erik A. Ranheim, Leonard I. Zon, and Emery H. Bresnick

Figure S1

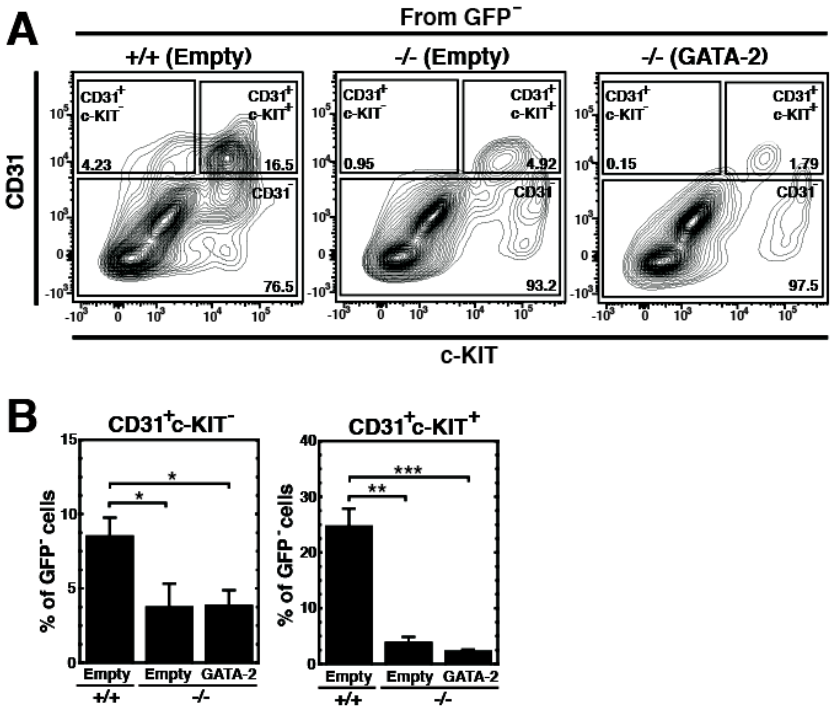

Figure S1. Related to Figure 1: Retroviral-mediated GATA-2 expression does not rescue CD31$^+$c-KIT$^+$ hematopoietic and CD31$^+$c-KIT$^-$ endothelial cells in the GFP$^-$ cell population. (A) Representative plots from flow cytometric analysis of CD31$^+$c-KIT$^+$ and CD31$^+$c-KIT$^-$ cell populations in GFP$^-$ cells after 96h of *ex vivo* culture. (B) Quantitation of flow cytometry data expressed as the percentage of CD31$^+$c-KIT$^-$ and CD31$^+$c-KIT$^+$ cells in GFP$^-$ cells (6 litters: +9.5$^{+/+}$-Empty [n=8 embryos]; +9.5$^{-/-}$-Empty [n=4 embryos]; +9.5$^{-/-}$-GATA-2 [n=6 embryos]). Error bars represent SEM. *, $P < 0.05$; **, $P < 0.01$; ***, $P < 0.001$ (two-tailed unpaired Student's t-test).

Figure S2

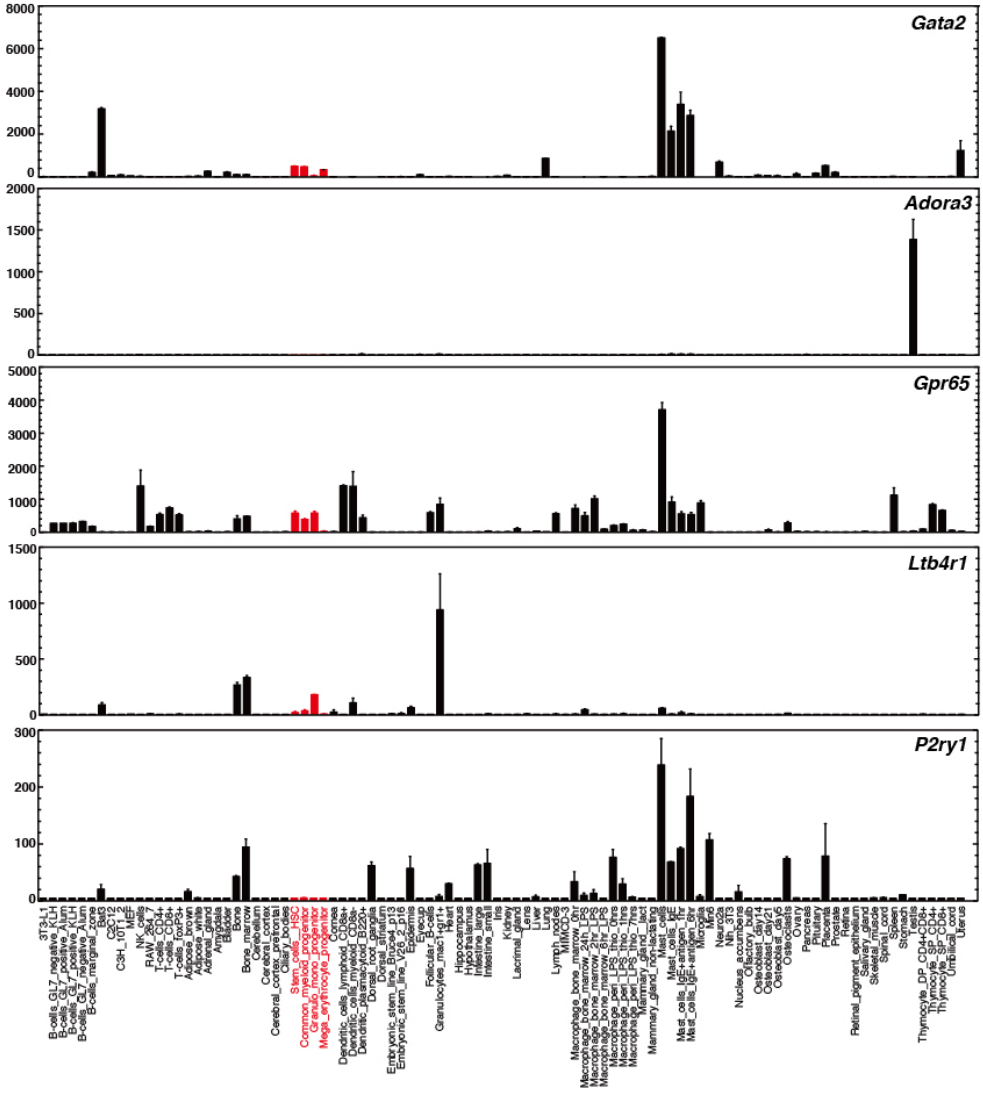

Figure S2. Related to Figure 3: Expression profiles from normal mouse tissues, organs, and cell lines (biogps.org).

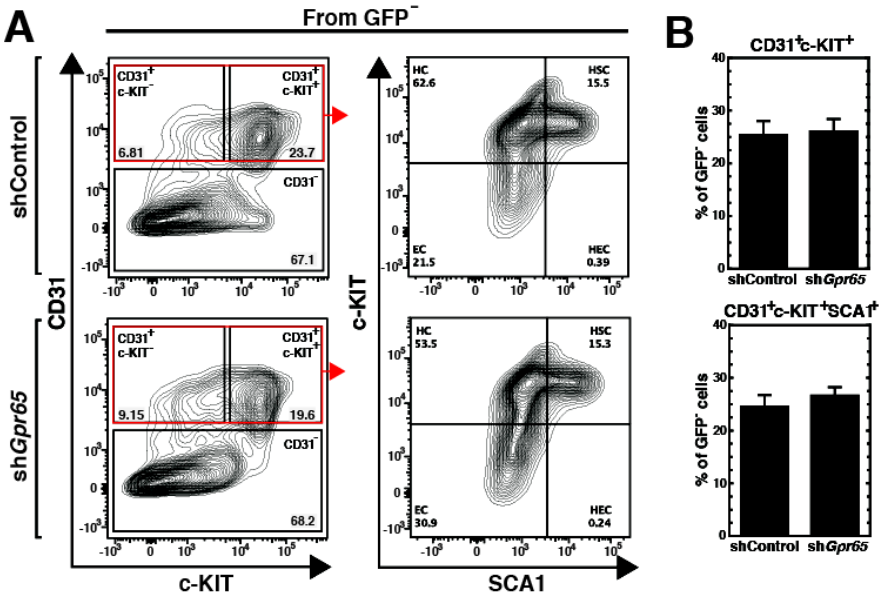

Figure S3. Related to Figure 4: Retroviral-mediated shGPR65 expression does not alter the CD31$^+$c-KIT$^+$ and CD31$^+$c-KIT$^+$SCA1$^+$ cell populations in the GFP$^-$ cell population. (A) Representative plots from flow cytometric analysis of CD31$^+$c-KIT$^+$ and CD31$^+$c-KIT$^+$SCA1$^+$ cell populations in GFP$^-$ cells after 96 h of culture. (B) Quantitative analysis of flow cytometry data expressed as the percentage of CD31$^+$c-KIT$^+$ and CD31$^+$c-KIT$^+$SCA1$^+$ cells in GFP$^-$ cells (Top: 9 litters: shLuc [n=22 embryos], sh*Gpr65* [n=26 embryos]; Bottom: 7 litters: shLuc [n=18 embryos]; sh*Gpr65* [n=22 embryos]).

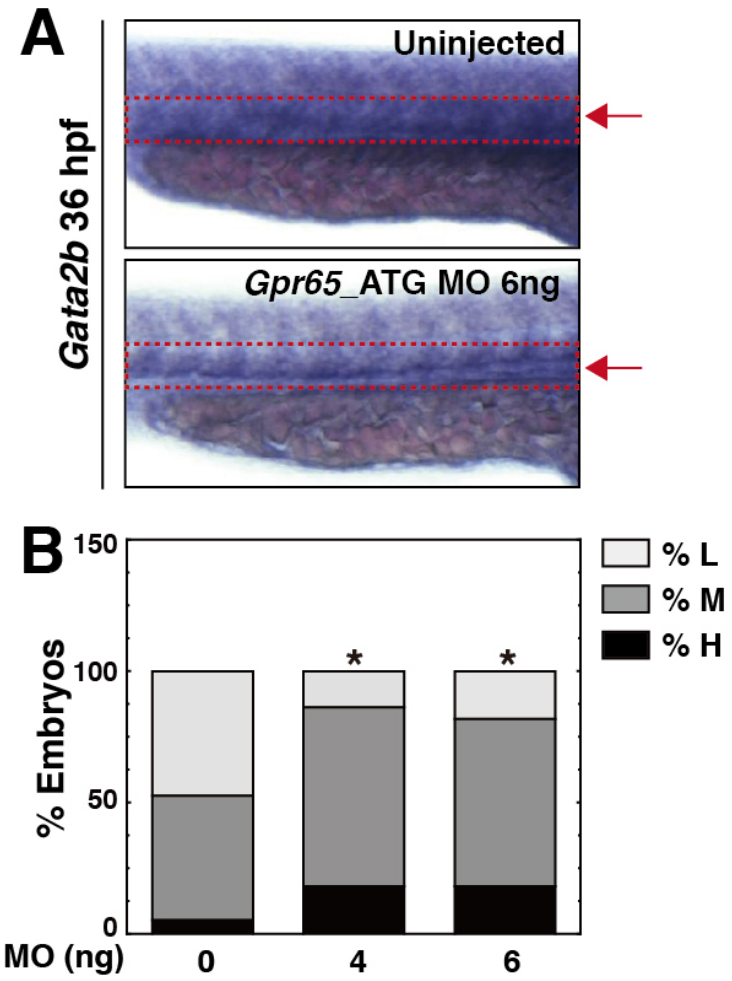

Figure S4. Related to Figure 5: GPR65 suppresses *Gata2* expression in the zebrafish embryo. (A) Representative images of in situ hybridization for *Gata2* at 36 hours post fertilization. The red rectangle illustrates the region enriched in hemogenic endothelium. (B) Quantitative analysis of in situ hybridization data expressed as percentage of embryos with high, medium, and low *Gata2* staining in total embryos (ATG_MO 0ng [n=104 embryos]; ATG_MO 4ng [n=22 embryos]; ATG_MO 6ng [n=40 embryos]). Error bars represent SEM. *, $P < 0.05$ (two-tailed unpaired Student's t-test).

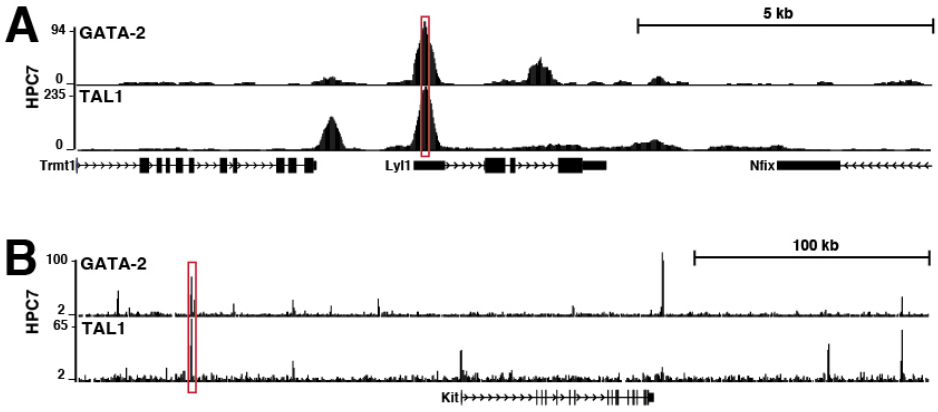

Figure S5. Related to Figure 6: ChIP-seq analysis of GATA-2 and TAL1 occupancy at Lyl1 (A) and KIT (B) loci in HPC7 cells. The red box depicts the amplified sequence from the real-time RT-PCR analysis of Figure 6K.

Supplemental Experimental Procedures

Primary erythroid precursor cell isolation. Primary erythroid precursors were isolated from E14.5 fetal livers using the EasySep negative selection Mouse Hematopoietic Progenitor Cell Enrichment kit (StemCell Technologies) (Hewitt et al., 2015; McIver et al., 2014). Fetal livers were dissociated by pipetting and resuspended at 5 x 10^7 cells/ml in PBS containing 2% FBS, 2.5 mM EDTA, and 10 mM glucose. EasySep Mouse Hematopoietic Progenitor Cell Enrichment Cocktail was added at 50 µg/ml supplemented with 2.5 µg/ml biotin-conjugated CD71 antibody (eBioscience). After 15 min incubation on ice, the cells were washed by centrifugation for at 1200 rpm at 4°C. Cells were resuspended at 5 X 10^7 cells/ml in PBS containing 2% FBS, 2.5 mM EDTA, and 10 mM glucose, and EasySep Biotin Selection Cocktail was added at 100 µg/ml. After 15 min incubation at 4°C, EasySep Mouse Progenitor Magnetic Microparticles were added at 50 µg/ml. After 10 min incubation at 4°C, cells were resuspended to 2.5 ml and incubated with a magnet for 3 min. Unbound cells were carefully transferred into 15 ml tube and used for subsequent experiments.

Cell culture. G1E-ER-GATA-1 cells were cultured with or without 1 µM estradiol as described (DeVilbiss et al., 2013). Fetal liver erythroid precursor cells were cultured and maintained at a density of 2.5 x 10^5 – 1 x 10^6 cells/ml in StemPro-34 (Gibco) supplemented with 10% nutrient supplement (Gibco), 2 mM L-glutamine (Cellgro), 1% penicillin/streptomycin (Cellgro), 100 µM monothioglycerol (Sigma-Aldrich), 1 µM dexamethasone (Sigma-Aldrich), 0.5 U/ml of erythropoietin, and 1%

conditioned medium from a KIT ligand-producing CHO cell line for expansion. Cells were cultured in a humidified incubator at 37°C and 5% carbon dioxide.

Retroviral infection: For concentrating retrovirus, the retroviral supernatant was mixed with the Retro-X Concentrator and rotated at 4°C for 1h. The mixture was then centrifuged at 1,500 g for 45 minutes to obtain a high-titer virus-containing pellet that was resuspended at 1% of the original volume in IMDM Media supplemented with 20% FBS [Gemini] and 1% penicillin/streptomycin [Cellgro].

Gpr65 shRNA sequence:

TGCTGTTGACAGTGAGCGAGCAGGTTAAGTTACATGGTATTAGTGAAGCCA

CAGATGTAATACCATGTAACTTAACCTGCCTGCCTACTGCCTCGGA

Quantitative real-time RT-PCR. Total RNA was purified from TRIzol (Invitrogen) according to manufacturers' instructions. cDNA was synthesized from 1 μg purified total RNA by Moloney murine leukemia virus reverse transcriptase (M-MLV RT). Real-time PCR was performed with SYBR green master mix (Applied Biosystems), and product accumulation was monitored by SYBR green fluorescence using either a StepOnePlus or Viia7 instrument (Applied Biosystems). Relative expression was determined from a standard curve of serial dilutions of cDNA samples, and values were normalized to 18S RNA expression. The sequences of primers used for RT-PCR and genotyping are provided below.

Colony assay. FACS-sorted $CD31^{+}$c-KIT^{+} cells from infected AGMs were plated in MethoCult M03434 complete media (StemCell Technologies) in a 35mm dish. After incubation in a humidified incubator at 37°C with 5% carbon dioxide,

colonies were visualized by microscopy and quantitated. Cells isolated from colonies were subjected to Wright-Giemsa staining.

Flow cytometry. Antibodies used for flow cytometry: APC-conjugated antibody CD31 (MEC13.3, Biolegend), PE-conjugated antibody c-KIT (2B8, eBioscience), PerCP-Cy5.5-conjugated antibody SCA1 (D7, eBioscience), APC-conjugated antibody Ter119 (TER119, eBioscience) and PE-conjugated CD71 (R17217, eBioscience) were used for flow cytometry and Fluorescence Activated Cell Sorting (FACS).

Dissociated cells from cultured AGM explants were resuspended in PBS containing 2% FBS and passed through 25 μm cell strainers to obtain single-cell suspensions prior to antibody staining. Fetal liver cells were washed with PBS once prior to antibody staining. Samples were analyzed on a FACSAria™ II cell sorter (BD Biosciences). Cells were gated on GFP to ensure retroviral expression. DAPI (Sigma-Aldrich) exclusion was utilized for live/dead discrimination. FACS-sorted cells were immediately processed for RNA isolation or colony assay.

Zebrafish morpholino knockdown. Detailed methodology is presented in supplemental experimental procedures.Wild-type zebrafish embryos were injected at the single cell stage with 0, 4, or 6 ng of *Gpr65*_ATG MO (MO sequence: CATCTCAAGGGAGCATAAGTGCGTC) or *Gpr65*_SP MO (MO sequence: TAAATCGACAACTCACCATAAGTGC). Embryos were grown to 36 hours post-fertilization. No defects in gross morphology or circulation were noted at the MO doses used. Embryos were fixed in formaldehyde and stained by *in*

situ hybridization with either a *Gata2b* probe or a *runx1/c-myb* probe mixture. Embryos were blindly scored as having either low, medium, or high AGM expression of *runx1/c-myb or Gata2b*. The *Gata2b* probe was generously provided by David Traver.

ChIP assay. Detailed methodology is presented in supplemental experimental procedures. Quantitative chromatin immunoprecipitation (ChIP) was conducted as described using antibodies specific to monomethylated H4K20 (Millipore), GATA-1, and Scl/TAL1 (DeVilbiss et al., 2015). Samples were analyzed by quantitative real-time PCR using either a StepOnePlus or Viia7 instrument (Applied Biosystems). The amount of product was determined relative to a standard curve generated from a serial dilution of input chromatin.

Primers.

+9.5 flanking forward: 5′-ATGTCCTTTCGGATCTCCTGCC-3′

+9.5 flanking reverse: 5′-GGTAAACAGAGCGCTACTCCTGTGTGTT-3′

18S rRNA forward: 5’-CGCCGCTAGAGGTGAAATTCT-3’

18S rRNA reverse: 5’-CGAACCTCCGACTTTCGTTCT-3’

Gata2 mRNA forward: 5′-GCAGAGAAGCAAGGCTCGC-3′

Gata2 mRNA reverse: 5′-CAGTTGACACACTCCCGGC-3′

Gpr65 mRNA forward: 5’-CAAGAGAAGCATCCCTCCAGAA-3’

Gpr65 mRNA reverse: 5’-TGTTTTTATTTTCACGCCGTTTG-3’

Gata2 primary transcript forward: 5’-GACATCTGCAGCCGGTAGATAAG-3’

Gata2 primary transcript reverse: 5’-CATTATTTGCAGAGTGGAGGGTATTAG-3’

MyoD promoter forward: 5′-GGGTAGAGGACAGCCGGTGT-3’

MyoD promoter reverse: 5′-GTACAATGACAAAGGTTCTGTGGGT-3’

Eif3k promoter forward: 5′-GTGATTTCCTTCCAGCAGTTGTAA-3’

Eif3k promoter reverse: 5′-CTCACGCTATTGGTCTCTTTTAAGTG-3’

Gata2 _9.5 Site _933 bp forward: 5′-CTTGCTGCTGGCTCTGAGAAC-3’

Gata2 _9.5 Site _933 bp reverse: 5′-AGTCCAGGGTCTTTTAAGGATAAATTC-3’

Gata2 _9.5 Site_480 bp forward: 5′-AACCTTCAAATGCAGACACTTCAC-3’

Gata2 _9.5 Site_480 bp reverse: 5′-GAATCCGCCAGAACGAAGAC-3’

Gata2_9.5 Site forward: 5′-GACATCTGCAGCCGGTAGATAAG-3’

Gata2_9.5 Site reverse: 5′-CATTATTTGCAGAGTGGAGGGTATTAG-3’

Gata2_9.5 Site_446 bp forward: 5′-GCCGAGGGAGTTCAGTGCTA-3’

Gata2_9.5 Site_446 bp reverse: 5′-AGCGCTACTCCTGTGTGTTCTTC-3’

Gata2_9.5 Site_880 bp forward: 5′-TCCTGGCGACTCCTAGATCCTA-3’

Gata2_9.5 Site_880 bp reverse: 5′-GAAAGCCCTGAGGAAGTTGGA-3’

Lyl1 Exon 1 forward: 5′-TCAGCATTGCTTCTTATCAGCC-3’

Lyl1 Exon 1 reverse: 5′-CGCAGAGGCCAGAGGATG-3’

Kit_114 kb forward: 5′-GCACACAGGACCTGACTCCA-3’

Kit_114 kb reverse: 5′-GTTCTGAGATGCGGTTGCTG-3’

Hdc mRNA forward: 5’-ACCTCCGACATGCCAACTCT-3’

Hdc mRNA reverse: 5’-CCGAATCACAAACCACAGCTT-3’

c-Kit mRNA forward: 5’-AGCAATGGCCTCACGAGTTCTA-3’

c-Kit mRNA reverse: 5’-CCAGGAAAAGTTTGGCAGGAT-3’

Lyl1 mRNA forward: 5’-AAGCGCAGACCAAGCCATAG-3’

Lyl1 mRNA reverse: 5’-AGCGCTCACGGCTGTTG-3’

c-Myb mRNA forward: 5’-CGAAGACCCTGAGAAGGAAA-3’

c-Myb mRNA reverse: 5’-GCTGCAAGTGTGGTTCTGTG-3’

Runx1 mRNA forward: 5’-TCACTGGCGCTGCAACAA-3’

Runx1 mRNA reverse: 5’-TCTGCCGAGTAGTTTTCATCGTT-3’

TAL1 mRNA forward: 5’-GAGGCCCTCCCCATATGAGA-3’

TAL1 mRNA reverse: 5’-GCGCCGCACTACTTTGGT-3’

Sfpi1 mRNA forward: 5’-GGCAGCGATGGAGAAAGC-3’

Sfpi1 mRNA reverse: 5’-GGACATGGTGTGCGGAGAA-3’